The Pennsylvania State University

The Graduate School

Department of Chemistry

A COMPUTATIONAL STUDY OF THE DISSOLUTION OF ALUMINOSILICATE MINERALS

A Thesis in

Chemistry

by

Christin E. Palombo

Submitted in Partial Fulfillment

of the Requirements

for the Degree of

Master of Science

December 2008

The thesis of Christin E. Palombo was reviewed and approved* by the following:

Barbara J. Garrison
Shapiro Professor of Chemistry
Thesis Adviser

Nicholas Winograd
Evan Pugh Professor of Chemistry

Sharon Hammes-Schiffer
Eberly Professor of Biotechnology

Ayusman Sen
Professor of Chemistry
Head of the Department of Chemistry

*Signatures are on file in the Graduate School.

ABSTRACT

The reactions of aluminosilicate clusters with water are investigated using ab-initio calculations. Reaction mechanisms for silicon terminated, Si-O_{br}-Al, sites as well as aluminum terminated, Al-O_{br}-Si, sites were determined using B3LYP/6-311+G(d,p) calculations. The calculated barrier heights for protonated and neutral Al-O_{br}-Si sites are predicted to be lower than those for Si-O_{br}-Si and Si-O_{br}-Al sites which mimics the dissolution of these minerals, and the Si-O_{br}-Al dissolution reactions proceeded in fundamentally the same fashion as those for Si-O_{br}-Si [S. Nangia and B. J. Garrison, *J. Phys. Chem. A* **2008**, *112*, 2027]. The barrier heights for the rate determining step for these reactions are calculated using the B3LYP, PBE1PBE, and M05-2X functionals in combination with the 6-311+G(d,p) and MG3S basis sets, and trends seen in the mechanistic calculations are repeated with each computational method.

TABLE OF CONTENTS

LIST OF FIGURES

LIST OF TABLES

ACKNOWLEDGEMENTS

I would first like to thank Barbara for instigating my graduate career. I was inspired to attend graduate school early in my undergraduate career after listening to a seminar Barbara gave at a conference I attended, and because of her, I realized how fascinating science can be. I have learned so much from her guidance and support as my advisor over the last four years.

I would like to thank Shikha for being my research partner. I piggy-backed onto a project which she started, and in her truest sense of character, she welcomed me as an equal and gladly showed me the ropes. Shikha, I am greatly indebted to you, and I have discovered an amazing world of kinetics and a sense of scientific judgment which are priceless qualities that will carry me far. It was truly my pleasure to work with you.

In no way would this Master's thesis be possible without my fiancée, Tom. He always knew when to be a colleague and when to be a friend. I have greatly benefitted from our dinnertime conversations as well as all the support he gave me during those long days and nights when I thought this day would never come.

I would also like to thank the members of the Garrison group, current and past, who pushed me along during my time with them. In particular, I would like to thank Dr. Chris Szakal, Dr. Pat Conforti, and the very-near-future Dr. Mike Russo. Chris, Pat, and Mike provided guidance during my orals, helped me in the earliest part of my career particularly when I crashed the group computer, and in my decision to change research groups. Their down-to-earth nature as well as awesome talent for science research are an inspiration to me and a great compliment to them.

Lastly, I have to thank my tireless team of cheerleaders who include family and friends alike. My parents, Aldo and Mary Pat; my sisters, Kim and Regina; and my aunts, Kathleen Ward Brown and Sandi Palombo, who knew that I could do it and helped me to remember that I should never give up. Raysun Goergen and my “fellow” graduate students in the Chemistry Department as well as other departments here at Penn State were also with me every step of the way. You know who you are, and I am forever grateful.

This work is dedicated to my grandparents, Patrick and Elizabeth Ward and Aldo and Sylvia Palombo, for teaching me how to work hard and showing me the courage to keep going.

Chapter 1: Introduction

The continual change of Earth's crust is in part affected by the competing processes of dissolution and precipitation, and thus dissolution is one fraction of the dynamic synergy controlling Earth's landscape. In addition, the dissolution of minerals affects the global CO_2 concentration and groundwater chemistry[1] and is vital to the sustainability of biota.[2] Furthermore, the dissolution of some minerals has been linked to harmful health effects in animals[3] and humans.[4] For these reasons, analyses of mineral dissolution are imperative, and descriptions of reactions which occur during dissolution play a role in understanding the how the process proceeds and provide insight into applications of the process on a larger scale.

Investigations of reactions across all spatial scales are necessary to understand the behavior of Earth's crust,[2] but one challenge which faces researchers today is that measurements taken at one scale do not necessarily transfer to another scale.[5] Thus experimental models are constantly being developed, and alternative approaches to probe geologic systems are required for a deeper understanding of dissolution. Model experimental systems have been shown to mimic natural minerals in both chemical makeup and trends of dissolution,[6-8] and this knowledge enables computational chemists to choose the most relevant fractions of a mineral and study those in particular.[9,10] In previous analyses[9,11,12] of dissolution, the two reactions which have caught the most attention are the successive opening of the mineral network to expose sites which contain only one oxygen atom linking them to the surface as well as the breaking of that single bond to release surface species to solution.

A study of mechanisms for reactions during dissolution is necessary to determine how these reactions proceed and to provide insight for experimental observations. One observation which warrants additional investigation is that a layer develops on an aluminosilicate surface during dissolution which has decreased Na^+ and Al^{3+} concentrations,[13,14] but experimental probes[15-17] of activation energies (E_a) for these surfaces calculate values which include all sites on the surface without a focus on aluminum terminated sites to explain this observation. Therefore a systematic examination to determine both the mechanisms and barrier heights of reactions for dissolution of aluminosilicate minerals is required which includes both Si-O_{br}-Al and Al-O_{br}-Si sites.

Computational approaches to examine the dissolution of minerals include the same challenges of previous investigations[2,5] to replicate trends across spatial scales. The ability to mimic behavior in experimental studies as well as the integration of realistic representations of chemical processes are concerns one faces using theoretical methods. As with experiment, calculations can be designed to model various aspects of dissolution. Large scale computational methods which include hundreds to thousands of particles have examined several aspects of dissolution[18,19] or the structure of aluminosilicate glasses[20-22] which are models for aluminosilicate minerals.[7] However, the investigation of site-specific reactions requires methods used for the determination of reaction mechanisms[10] which can be included in computational analyses of dissolution using bulk-like systems.[12,23]

The use of small clusters in ab-initio calculations is one approach to model reactions which occur during dissolution, and reaction mechanisms are determined that

explain observations or replicate trends seen in experiment.[10,24-27] Despite the size difference between model clusters and experimental systems, this approach has been successful for quartz,[10] and here a similar methodology is tested for aluminosilicate systems.

The work presented in the following chapters incorporates dissolution reaction mechanisms for silicon and aluminum terminated sites on aluminosilicate mineral surfaces and includes the various protonation states possible on a mineral surface as well as the coordination changes of aluminum. Chapter 2 examines the various computational methods used for dissolution studies, and an explanation is given of why the ab-initio approach chosen here is appropriate for the systems investigated. The dissolution reaction analysis follows in Chapter 3 where reaction mechanisms are determined, and several ab-initio methods are compared. The conclusion in Chapter 4 summarizes the study given here and gives several possible future directions.

References

(1) Brantley, S. L. Kinetics of mineral dissolution. In *Kinetics of Water-Rock Interaction*; Brantley, S. L., Kubicki, J. D., White, A. F., Eds.; Springer: New York, NY, 2008; pp 151.

(2) Brantley, S. L.; Goldhaber, M. B.; Ragnarsdottir, K. V. *Elements* **2007**, *3*, 307.

(3) Birchall, J. D.; Exley, C.; Chappell, J. S.; Phillips, M. J. *Nature* **1989**, *338*, 146.

(4) Swaddle, T. W. *Coordination Chemistry Reviews* **2001**, *219*, 665.

(5) Navarre-Sitchler, A.; Brantley, S. *Earth and Planetary Science Letters* **2007**, *261*, 321.

(6) Hamilton, J. P.; Pantano, C. G.; Brantley, S. L. *Geochimica et Cosmochimica Acta* **2000**, *64*, 2603.

(7) Hamilton, J. P.; Brantley, S. L.; Pantano, C. G.; Criscenti, L. J.; Kubicki, J. D. *Geochimica et Cosmochimica Acta* **2001**, *65*, 3683.

(8) Tsomaia, N.; Brantley, S. L.; Hamilton, J. P.; Pantano, C. G.; Mueller, K. T. *American Mineralogist* **2003**, *88*, 54.

(9) Criscenti, L. J.; Brantley, S. L.; Mueller, K. T.; Tsomaia, N.; Kubicki, J. D. *Geochimica et Cosmochimica Acta* **2005**, *69*, 2205.

(10) Nangia, S.; Garrison, B. J. *Journal of Physical Chemistry A* **2008**, *112*, 2027.

(11) Casey, W. H.; Westrich, H. R.; Arnold, G. W.; Banfield, J. F. *Geochimica et Cosmochimica Acta* **1989**, *53*, 821.

(12) Nangia, S.; Garrison, B. J. *Geochimica et Cosmochimica Acta* **2008**, submitted.

(13) Hellmann, R.; Eggleston, C. M.; Hochella, M. F., Jr.;; Crear, D. A. *Geochimica et Cosmochimica Acta* **1990**, *54*, 1267.

(14) Stillings, L. L.; Brantley, S. L. *Geochimica et Cosmochimica Acta* **1995**, *59*, 1483.

(15) Hellmann, R. *Geochimica et Cosmochimica Acta* **1994**, *58*, 595.

(16) Chen, Y.; Brantley, S. L. *Chemical Geology* **1997**, *135*, 275.

(17) Blum, A. E.; Stillings, L. L. Feldspar dissolution kinetics. In *Chemical Weathering Rates of Silicate Materials*; White, A. F., Brantley, S. L., Eds.; Mineralogical Society of America: Washington, D. C., 1995; Vol. 31; pp 291.

(18) Spagnoli, D.; Kerisit, S.; Parker, S. C. *Journal of Crystal Growth* **2006**, *294*, 103.

(19) Mahadevan, T. S.; Garofalini, S. H. *Journal of Physical Chemistry C* **2008**, *112*, 5694.

(20) Zirl, D. M.; Garofalini, S. H. *Journal of the American Ceramic Society* **1990**, *73*, 2848.

(21) Montosri, M.; Menziani, M. C.; Leonelli, C.; Cormack, A. N. *Molecular Engineering* **1999**, *8*, 427.

(22) Ganster, P.; Benoit, M.; Kob, W.; Delaye, J. M. *Journal of Chemical Physics* **2004**, *120*, 10172.

(23) Lasaga, A. C. Fundamental approaches in describing mineral dissolution and precipitation rates. In *Chemical Weathering Rates of Silicate Minerals*; Brantley, S. L., White, A. F., Eds.; Mineralogical Society of America: Washington, D. C., 1995; Vol. 31; pp 27.

(24) Xiao, Y.; Lasaga, A. C. *Geochimica et Cosmochimica Acta* **1994**, *58*, 5379.

(25) Xiao, Y.; Lasaga, A. C. *Geochimica et Cosmochimica Acta* **1996**, *60*, 2283.

(26) Casey, W. H.; Swaddle, T. W. *Reviews of Geophysics* **2003**, *41*, 1008.

(27) Helm, L.; Merbach, A. E. *Chemical Reviews* **2005**, *105*, 1923.

Chapter 2: Modeling Mineral Dissolution

2.1 Choosing the Best Computational Method

The analysis of chemical processes using computational methods requires a balance between the size of the system and the quantum resolution represented. When a chemical process is modeled with a large number of atoms, for example $10^2 - 10^5$, the electronic structure cannot be included for all the particles because this evaluation would be too computationally intensive; therefore, large scale calculations would require approximations of electronic behavior. The description of quantum effects during a chemical process can be made by evaluating the behavior of a small number of atoms, typically less than 50. Several of the popular classes of computational methods will be described here to show for which types of systems these methods can be used, and an explanation of why the employment of model clusters is effective to describe chemical processes is also included.

The computational methods outlined here are presented in order from largest to smallest possible system, and an application of each is included. For systems with hundreds[1-3] to thousands of particles,[4,5] molecular dynamics (MD) simulations are a useful tool. Using Newton's second law, the positions and velocities of each particle are tracked with time, and potentials to describe the means by which each particle will interact with one another are used in the system.[6] The evaluation of vibrational motion, Coulombic and Lennard-Jones interactions, and van der Waals interactions are included.[7] There are many possible applications of MD simulations, and two which are relevant to

mineral dissolution are the examination of the structure of aluminosilicate glasses[1-3] as well as a model for the interaction of water with steps on a mineral surface.[4]

Monte Carlo (MC) simulations can be used for systems with a comparable size to those used in MD simulations, but unlike MD simulations, Monte Carlo simulations do not include a time parameter.[6] Instead, random configurations of particles in a system are evaluated in comparison with the energy of the previous configuration. If the current configuration is lower in energy than the previous one, then the system assumes the new configuration. If not, then two choices are possible. The Boltzmann factor, $e^{-\Delta E/k_B T}$, is used as a benchmark against a random number between zero and one. If the random number is greater than $e^{-\Delta E/k_B T}$, then the current configuration is adapted. If the random number is less than the Boltzmann factor, the previous configuration is maintained.[8] The absence of a time-related quantity in a Monte Carlo simulation allows for the examination of processes like dissolution[9,10] which can proceed over long time scales when studied experimentally.[11]

The last computational class of methods described here is ab-initio methods which evaluate chemical systems from a quantum perspective. Unlike the other methods discussed so far which account for the presence of electrons through the use of potentials or molecular geometries hard-wired into a program, ab-initio computational methods evaluate the behavior of electrons using approximations to the Schrodinger equation, and the geometries or energies calculated are a result of the quantum effects in the system or process. This type of calculation is effective for examining processes which include bond-breaking and bond-forming because electronic character is included explicitly.[6] Present day computational resources limit the number of atoms that may be included in a

calculation. The small size of the system allows for the use of model clusters which effectively represent the behavior of the bulk of the system[12] and enables the determination of barrier heights and mechanisms for dissolution.[12-14]

2.2 Determining an Appropriate Ab-Initio Method

The use of ab-initio methods to investigate dissolution reactions is oriented toward the representation of quantum effects in order to determine reaction mechanisms and barrier heights. Once the choice of an ab-initio approach has been made, the next question is which type of ab-initio method is appropriate. The method chosen must model the system effectively in terms of molecular geometry, accurate bonding character for each element, and computational feasibility, and both the functional and the basis set affect these quantities. Two classes of ab-initio methods exist: wave function theory (WFT) and density functional theory (DFT) methods. WFT methods have been shown to be more computationally intensive and require larger basis sets than DFT, and the electronic description present in DFT methods is also more accurate.[15] For these reasons, DFT will be used here.

A functional is the set of functions which describes the electronic character of a system in terms of the energy and electron density gradient.[8] Each of these quantities can be further partitioned, and a description of which functionals include each follows below. For any ab-initio calculation, a functional is combined with a basis set which refers to the collection of functions used to describe the orbitals on each atom, and basis sets can be partitioned to describe core and valence electrons separately.[8] The decision of which ab-

initio method to choose requires consideration of each of these quantities in its application to the chemical system and analysis at hand.

In addition to considerations regarding the chemical process which will be studied with ab-initio methods, the representation of several phenomena which describe chemical behavior in ab-initio calculations must reflect the system under study accurately, and therefore a number of concepts on which ab-initio methods are based will be defined here. Electron-exchange is the energy which arises when two electrons are inverted in the wavefunction description of electrons,[7,16] and normally this quantity relates electrons of the same spin.[17] Often coupled with the electron exchange term, the electron correlation describes the physical phenomenon where the motion of each electron is related to the motion of every other electron in the system,[7,18] and this quantity relates electrons of the opposite spin.[17] Lastly, exchange-correlation is the combination of electron exchange and correlation terms present in the energy description of electrons.[7,17]

In terms of applying the exchange-correlation to a functional, each description of either the electron exchange or the electron correlation can be improved to represent electronic structure more efficiently. Three quantities which are used to do this are Hartree-Fock exchange, the generalized gradient approximation, and the kinetic energy density. The Hartree-Fock (HF) exchange is the exact treatment of electron exchange in accordance with the Hartree-Fock theory,[19] and this is used to supplement the exchange-correlation terms in more simplistic functionals. The generalized gradient approximation (GGA) is the weighting of the change of electron density in the exchange and correlation functions,[8] and this serves to improve the performance over previous methods in the ability to represent bonds better and calculate barrier heights more effectively.[17] Lastly,

the kinetic energy density, which is the kinetic energy of electrons within a given volume,[7] has been included in some recent ab-initio methods[20] and has been useful in the determination of barrier heights.[17]

As the functional describes the electronic energy, the basis set describes the atomic orbitals on each atom, and there are two classes of orbitals: Gaussian type orbitals (GTOs) and Slater type orbitals (STOs). Both STOs and GTOs include an exponential dependence upon the distance between the electron and the nucleus, but for GTOs, this distance is more heavily weighted. In GTOs, therefore, regions close to and far from the nucleus suffer from an insufficient description, and to suffice, more GTOs are needed to describe electronic behavior than STOs for the same system. However, the increased number of functions as well as the simplistic form of the integrals have benefits. The additional functions allow for a more adaptable description of orbitals, and GTO-structured basis sets are more computationally feasible.[8]

GTOs used to describe the atomic orbitals of each atom are assembled, and the full set of functions is known as primitive Gaussian type orbitals or PGTOs. These PGTOs can be separated into those that describe core electrons and those that describe valence electrons, and this delineation is known as a split valence basis set. Split valence basis sets are defined by *k-nlmG*, to use Jensen's notation.[8] The first digit is the number of PGTOs used for core orbitals. The valence orbitals are described by the *nlm* fragment which splits valence into electrons described by *n*, *l*, and *m* numbers of PGTOs. Diffuse functions are used for anions or excited states where electrons are not held tightly by the nucleus, and the notation for these functions is a "+" sign. Polarization functions provide an additional description of electrons in regions other than the bond between two atoms

and are denoted "(x,y)" after the "G" in the basis set name.[8] Two examples of basis sets which include all of these quantities are the 6-311+G(d,p) basis set[21,22] and the MG3S basis set which is comprised of the 6-311+G(2df,2p) for hydrogen, the 6-311++G(2df,2p) for first row elements, and the 6-311+G(3d2f) for sodium, magnesium, aluminum, and silicon and resembles the 6-311+G(3d2f) for phosphorus, sulfur, and chlorine.[23]

Many types of ab-initio methods exist, and each one has a strength for a given application. The inclusion of both exchange and correlation is standard practice,[17] and all of the functionals used in the following chapter have this quantity. DFT methods partition electronic energy into kinetic energy, electron-nuclear interaction, Coulomb repulsion, and exchange-correlation,[18] and the three methods in the next chapter are all examples of DFT ab-initio methods: B3LYP, PBE1PBE, and M05-2X and include a percentage of HF exchange. The use of DFT functionals is extensive[17] and shows that ab-initio methods which include an exchange-correlation constituent are much more popular than the exchange-only HF functional.

2.3 Building Upon Previous Studies

The use of small clusters in theoretical calculations focuses on the most fundamental aspects of a chemical process. Cluster-sized examinations of reactions occurring during dissolution allow for an understanding of dissolution on a molecular scale as well as for an analysis of specific surface sites.[12-14] Despite the molecular scale, the inclusion of additional non-reacting sites is not necessary because dissolution of surface sites has been shown to be independent of contributions from the bulk.[13] The knowledge gained can be applied to explain experimental observations and to shape

additional models of dissolution such as determination of dissolution rates[12] and descriptions of bulk-like systems.[24]

The use of model clusters to represent aluminosilicate minerals is employed here, and ab-initio calculations are performed to determine reaction mechanisms and barrier heights. The current study investigates the hydrolysis of Si-O_{br}-Al and Al-O_{br}-Si sites, where the leftmost element represents the terminal site, because experimental studies do not consider the contribution of individual types of sites on the activation energy (E_a) of dissolution of aluminosilicate minerals[25-27] as well as includes the protonation state of each site which affects the ease with which a site dissolves.[12-14] In addition, the model aluminosilicate clusters studied here include the various coordination states of an Al-O_{br}-Si sites on a surface[28-30] where a previous study included only a tetrahedral Al-O_{br}-Si site.[13] Further, these clusters are terminated with hydroxyl groups to simulate the bulk[12] and not hydrogen atoms.[13] Lastly, no previous work has evaluated the performance or computational intensity of a method for ab-initio calculations of an aluminosilicate system, and the investigation described in the following chapter includes all of these considerations.

References

(1) Zirl, D. M.; Garofalini, S. H. *Journal of the American Ceramic Society* **1990**, *73*, 2848.

(2) Montosri, M.; Menziani, M. C.; Leonelli, C.; Cormack, A. N. *Molecular Engineering* **1999**, *8*, 427.

(3) Ganster, P.; Benoit, M.; Kob, W.; Delaye, J. M. *Journal of Chemical Physics* **2004**, *120*, 10172.

(4) Spagnoli, D.; Kerisit, S.; Parker, S. C. *Journal of Crystal Growth* **2006**, *294*, 103.

(5) Mahadevan, T. S.; Garofalini, S. H. *Journal of Physical Chemistry C* **2008**, *112*, 5694.

(6) Leach, A. R. *Molecular Modeling: Principles and Applications*; Pearson Prentice Hall: New York, 2001.

(7) Atkins, P.; de Paula, J. *Physical Chemistry*, 7th ed.; W. H. Freeman and Company: New York, 2002.

(8) Jensen, F. *Introduction to Computational Chemistry*; John Wiley and Sons, Inc.: New York, 1998.

(9) Lasaga, A. C. Fundamental approaches in describing mineral dissolution and precipitation rates. In *Chemical Weathering Rates of Silicate Minerals*; Brantley, S. L., White, A. F., Eds.; Mineralogical Society of America: Washington, D. C., 1995; Vol. 31; pp 27.

(10) Lasaga, A. C.; Luttge, A. *European Journal of Mineralogy* **2003**, *15*, 603.

(11) Stillings, L. L.; Brantley, S. L. *Geochimica et Cosmochimica Acta* **1995**, *59*, 1483.

(12) Nangia, S.; Garrison, B. J. *Journal of Physical Chemistry A* **2008**, *112*, 2027.

(13) Xiao, Y.; Lasaga, A. C. *Geochimica et Cosmochimica Acta* **1994**, *58*, 5379.

(14) Xiao, Y.; Lasaga, A. C. *Geochimica et Cosmochimica Acta* **1996**, *60*, 2283.

(15) Zhang, Y.; Li, Z. H.; Truhlar, D. G. *Journal of Chemical Theory and Computation* **2007**, *3*, 593.

(16) Levine, I. N. *Quantum Chemistry*, 5th ed.; Prentice Hall: Upper Saddle River, 2000.

(17) Sousa, S. F.; Fernandes, P. A.; Ramos, M. J. *Journal of Physical Chemistry A* **2007**, *111*, 10439.

(18) Foresman, J. B.; Frisch, A. *Exploring Chemistry with Electronic Structure Methods*, 2nd ed.; Gaussian, Inc.: Pittsburgh, 1996.

(19) Becke, A. D. *Journal of Chemical Physics* **1993**, *98*, 1372.

(20) Zhao, Y.; Schultz, N. E.; Truhlar, D. G. *Journal of Chemical Theory and Computation* **2006**, *2*, 364.

(21) Krishnan, R.; Binkley, J. S.; Seeger, R.; Pople, J. A. *Journal of Chemical Physics* **1980**, *72*, 650.

(22) Clark, T.; Chandrasekhar, J.; Spitznagel, G. W.; von Rague Schleyer, P. *Journal of Computational Chemistry* **1983**, *4*, 294.

(23) Lynch, B. J.; Zhao, Y.; Truhlar, D. G. *Journal of Physical Chemistry A* **2003**, *107*, 1384.

(24) Nangia, S.; Garrison, B. J. *Geochimica et Cosmochimica Acta* **2008**, submitted.

(25) Hellmann, R. *Geochimica et Cosmochimica Acta* **1994**, *58*, 595.

(26) Blum, A. E.; Stillings, L. L. Feldspar dissolution kinetics. In *Chemical Weathering Rates of Silicate Materials*; White, A. F., Brantley, S. L., Eds.; Mineralogical Society of America: Washington, D. C., 1995; Vol. 31; pp 291.

(27) Chen, Y.; Brantley, S. L. *Chemical Geology* **1997**, *135*, 275.

(28) Martin, R. B. *Journal of Inorganic Biochemistry* **1991**, *44*, 141.

(29) Tsomaia, N.; Brantley, S. L.; Hamilton, J. P.; Pantano, C. G.; Mueller, K. T. *American Mineralogist* **2003**, *88*, 54.

(30) Swaddle, T. W.; Rosenqvist, J.; Yu, P.; Bylaska, E.; Philiips, B. L.; Casey, W. H. *Science* **2005**, *308*, 1450.

Chapter 3: Dissolution Mechanisms of Aluminosilicate Minerals using Ab-Initio Methods

3.1 Introduction

The dissolution of minerals is a ubiquitous process which occurs to some degree nearly everywhere on Earth and has an effect on a number of processes such as soil chemistry, water contaminants, and the global CO_2 cycle.[1] Aluminosilicate minerals are of particular importance because their primary constituents – namely aluminum, silicon, and oxygen – comprise the greatest percentage of the Earth's surface.[2] In addition, the presence of aluminum species in aqueous solution can be linked to serious health risks in humans[3] and other animals,[4] and this correlation, albeit controversial,[3] adds additional intrigue to the aluminosilicate dissolution.

The scheme shown in Fig. 1 depicts the arrangement of atoms in an aluminosilicate mineral. The surface appears as a dotted line in Fig. 1, and each Si or Al is terminated with hydroxyl groups to represent a generic site. Si terminated sites are called Si-O_{br}-Al here to indicate that the Si-O_{br} bond breaks to release Si species to solution, and similarly Al terminated sites are called Al-O_{br}-Si to indicate that the Al-O_{br} bond breaks. Each Al or Si from the surface is connected to the bulk via a bridging oxygen atom(O_{br}). The O_{br} is connected to another Al or Si where both exist in a tetrahedral bonding environment in the bulk.[5-7] However, additional configurations can be seen at surface sites, and a detailed explanation of such possibilities follows below.

The scheme of surface sites shown in Fig. 1 is overly simplistic because it does not take into account the protonation states of each site. Surface sites are referred to as

protonated, neutral, or deprotonated, and these terms describe whether the O_{br} is protonated or not, as in the neutral state. The deprotonated state is one where the O_{br} is not protonated, and one of the oxygen atoms from a surface hydroxyl group is missing an H^+, leaving that oxygen atom with a (–1) charge.

A recent description of quartz dissolution[8] includes the perspective that a mineral surface is comprised of a distribution of protonated, neutral, and deprotonated sites,[9] and a similar approach is adopted here. If one considers the schematic of an aluminosilicate mineral shown in Fig. 1, surface reactions at a site include interaction with the forms of Si sites shown in Fig. 2, where the bonding configuration of Al is meant to refer to the bulk of the mineral. The protonation states described above are shown, but these terms do not reflect the charge of each structure. Because quartz is an uncharged mineral, the charge of each site can be intuited from the name: protonated sites have a (+1) charge, neutral sites a (0) charge, and deprotonated sites a (–1) charge. For aluminosilicate minerals, this is not the case because the replacement of Si with Al in a tetrahedral bonding state brings a (–1) charge. Therefore, the protonated state for a Si-O_{br}-Al site has a (0) charge, while a neutral Si-O_{br}-Al site has a (–1) charge. Similarly, for deprotonated Si-O_{br}-Al sites, the charge is (–2). Thus even though each Si center maintains a tetrahedral bonding arrangement, the difference of a H^+ as well as the inclusion of an Al center opposite the O_{br} leads to charged protonation states.

The description of an Al-O_{br}-Si site on the surface is not as straightforward. Al is known to assume various coordination states[7] according to pH,[10,11] and thus an analysis of an Al-O_{br}-Si site on an aluminosilicate surface requires an awareness of the fact that a distribution of coordination states is possible on the surface. Therefore, the forms of

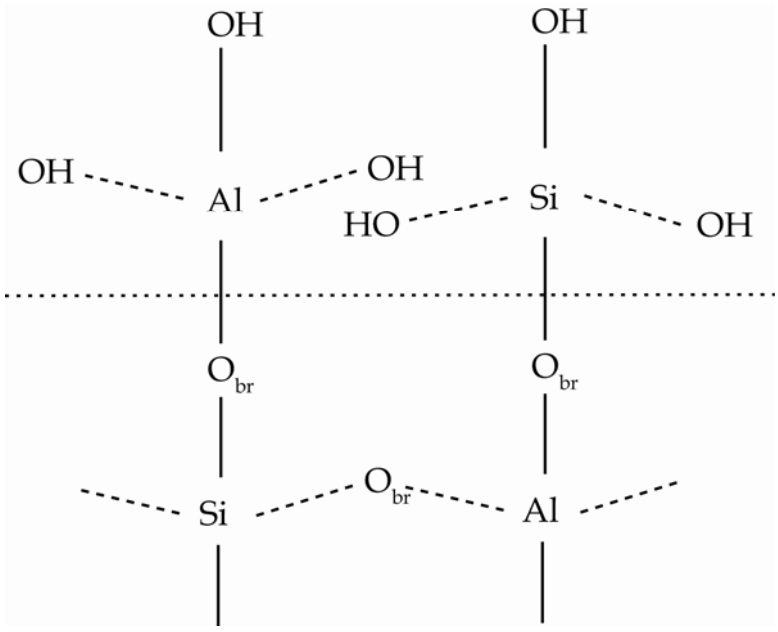

Figure 1: Schematic of aluminosilicate mineral. The surface is represented by the dotted line, and thus terminal sites may either be aluminum or silicon centers. Each site is bonded to a bridging oxygen atom to a neighboring aluminum or silicon atom.

Al-O_{br}-Si sites that can exist appear in Fig. 3, and the protonation states of each site are included. As with Si-O_{br}-Al sites, the terms of protonated, neutral, and deprotonated reflect the difference types of sites on the mineral surface and not the charge of the site.

The forms of Al-O_{br}-Si sites shown in Fig. 3 are reflect the possible coordination states of Al in solution, and this concept is included to show that a distribution of coordination states are also possible in the surface. In acidic pH ranges, Al is hexa-coordinated in solution,[10,11] and because a protonated site is the most prevalent type on a mineral surface in very acidic pH ranges,[12-14] a hexa-coordinated Al-O_{br}-Si site with a protonated O_{br} is an appropriate representation of a protonated site where Al is the terminal reaction center. This protonated site where Al is hexa-coordinated has a (+3) charge on an aluminosilicate surface. Using similar logic, Al is penta-coordinated in slightly acidic to neutral pH ranges,[10,11] and a neutral Al-O_{br}-Si site is represented by a penta-coordinated Al with a protonated O_{br}. Similar to the protonated site, a neutral site on an aluminosilicate surface has a (+3) charge. Lastly, Al is tetra-coordinated in basic pH ranges,[10,11] and thus a deprotonated Al-O_{br}-Si site can be represented by Al bonded to three hydroxyl groups and an O_{br}. The deprotonated site on an aluminosilicate surface has a (–1) charge. The protonated, neutral, and deprotonated sites have a charge because of the coordination capabilities of Al.

Although extensive analyses of the dissolution of aluminosilicate minerals have been published (see Blum and Stillings, 1995, for a review), no description of the dissolution reaction mechanism for these minerals has been presented. If one traces the dissolution of a particular aluminosilicate mineral, for example albite, the Na^+ and Al^{3+} leach from the mineral surface first,[15,16] and the Al^{3+} is replaced by H^+ ions from solution

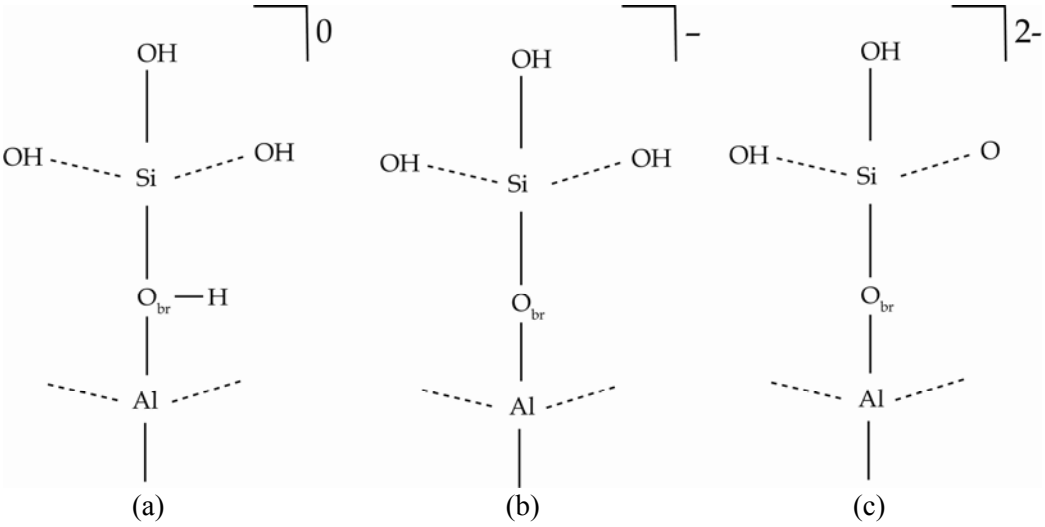

Figure 2: Schematic of Si sites possible on a surface. (a) Protonated. (b) Neutral. (c) Deprotonated.

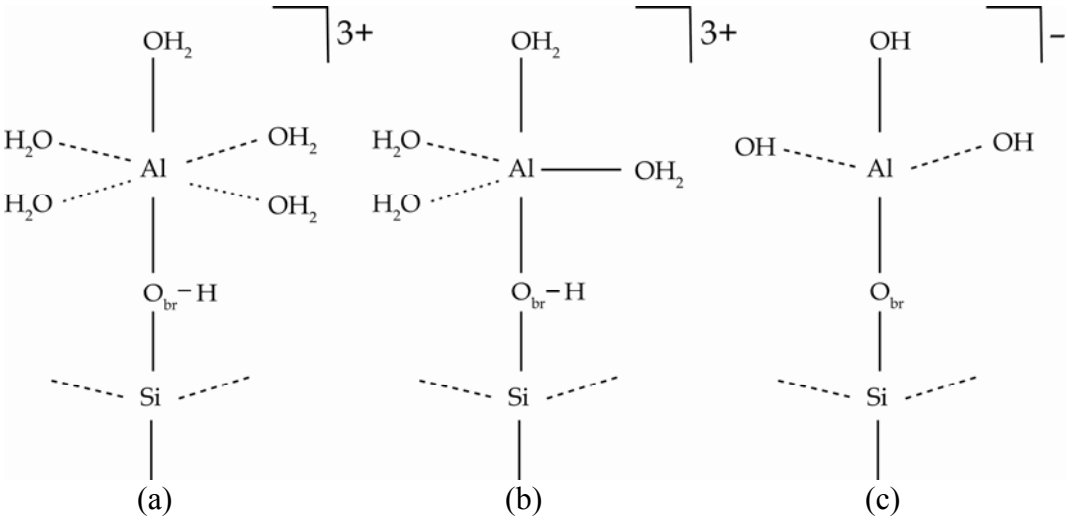

Figure 3: Schematic of Al sites possible on a surface. (a) Protonated. (b) Neutral. (c) Deprotonated.

during the leaching process.[6,15,17] These observations lead to several questions. The first is how the Al and Si species leave the surface; that is, how the Al-O_{br} or Si-O_{br} bonds break. Second, if charge-balancing cations have leached from the surface, then each site could have an inherent charge during the progression of a dissolution reaction, and comparison to dissolution reactions on the surface of quartz, a mineral devoid of charge-balancing cations, could give insight into the effect of charge on dissolution. Third, the development of a silica-rich layer during dissolution[17] shows that Al and Si must leach in different fashions which enable Al to leach first.

The final step is the release of the surface species into solution,[18] and because there are health effects related to Al species in solution,[3,4] the breaking of Al-O_{br} and Si-O_{br} bonds with aluminosilicate mineral surfaces is a particularly important process. At the surface, the terminal site is bonded to the surface solely via one bridging oxygen as in Figs. 2 and 3. This situation is a desirable place to begin a study of mineral dissolution because the energy barrier of this process is solely an effect of the release of the species from the surface. What is more, the knowledge gained from an understanding of how the final step in dissolution occurs would provide insight into how each species is released from the surface sequentially as well as how the leached layer develops on a surface.[17] In addition to differences in the means by which Al-O_{br}-Si and Si-O_{br}-Al sites dissolve, observed dissolution rates of aluminosilicate minerals at various pH values show a minimum at neutral pH[1] which could mean that different dissolution mechanisms exist.[6] Although dissolution in solution is a complex synergy of numerous processes, the focus here is the mechanism of the hydrolysis reaction with each type of site on a surface.

Ab-initio calculations have been shown as an effective method to determine mechanisms for reactions during dissolution as well as mimic trends seen in the field.[8] Previous studies have included either silaceous[8,19] or aluminum-containing[20,21] materials. Here the aluminosilicate system contains both elements, and thus one challenge will be to choose an ab-initio method appropriate to describe all the constituents present in this system. In an effort to encompass these concerns, several computational methods will be tested, and both the barrier heights calculated and the computational time used by each method will be compared.

3.2 Computational Method

3.2.1 Model Aluminosilicate Dissolution Reactions

Reactions at surface sites of aluminosilicate minerals with water are modeled using clusters depicted in Figs. 2 and 3 in an effort to understand the dissolution of these minerals. The use of model clusters to simulate the dissolution of minerals has been previously reported.[6,8,18,22,23] The reacting site is either Si-O_{br}-Al or Al-O_{br}-Si, and the cluster is terminated by hydroxyl groups for the bulk. The progression of the reaction is such that a water molecule approaches the reacting center, the bond between the reacting center and the O_{br} is broken, and the products represent the species released to solution and remaining surface constituents.

To model dissolution for Si-O_{br}-Al sites, the following three reactions were studied, and Eq. 1–3 represent the protonated, neutral, and deprotonated Si-O_{br}-Al sites, respectively.

$$[Si(OH)_3(O_{br}H)Al(OH)_3] + H_2O \rightarrow Si(OH)_4 + [Al(OH)_3(H_2O)] \quad (1)$$

$$[Si(OH)_3O_{br}\,Al(OH)_3]^- + H_2O \rightarrow Si(OH)_4 + [Al(OH)_4]^- \quad (2)$$

$$[(Si(OH)_2O)O_{br}Al(OH)_3]^{2-} + H_2O \rightarrow Si(OH)_3O^- + [Al(OH)_4]^- \quad (3)$$

Here the bond between O_{br} and Si breaks to release a Si species to solution and leave the O_{br} as one of the terminal O atoms bonded to Al in the products given here.

Protonated, neutral, and deprotonated Al-O_{br}-Si sites are given in Eq. 4–6 and include the coordination changes of Al with pH.[10,11]

$$[Al(H_2O)_5(O_{br}H)Si(OH)_3]^{3+} + H_2O \rightarrow [Al(H_2O)_6]^{3+} + Si(OH)_4 \quad (4)$$

$$[Al(H_2O)_4(O_{br}H)Si(OH)_3]^{3+} + H_2O \rightarrow H_3O^+ + [Al(OH)_2(H_2O)_2]^+ + Si(OH)_3(H_2O)^+ \quad (5)$$

$$[Al(OH)_3O_{br}Si(OH)_3]^- + H_2O \rightarrow [Al(OH)_3(H_2O)] + Si(OH)_3O^- \quad (6)$$

Similar to the Si-O_{br}-Al sites, the bond between Al and O_{br} breaks to release an Al species to solution, while the O_{br} remains on the Si center.

Because quartz is a neutral mineral, there was no need for charge-balancing cations in a recent investigation[8] into reaction mechanisms for dissolution of this mineral. Furthermore, Kubicki, et al. showed that the presence of Na^+ has a negligible effect on aluminosilicate clusters.[24] The goals here are to show how the final step of dissolution occurs – that is, the breakage of the Al-O_{br} or Si-O_{br} bond and the subsequent release of the relevant species into solution – and to calculate mechanisms which fit into the picture painted by previous researchers.[8,21] In the present work, charges on the clusters are maintained in the calculation, but no explicit charge-balancing cations are used.

3.2.2 Functionals and Basis Sets Used

Density functional theory (DFT) methods incorporate exchange-correlation into the functional as well as fragment the electron energy into quantities whose evaluation

can be performed within a reasonable computation time.[25] The reaction profiles of dissolution reactions for quartz surface sites have been examined using a DFT method, and experimental data were successfully explained.[8] For this reason, the use of the B3LYP functional here to model the dissolution of aluminosilicate minerals is appropriate. The B3LYP hybrid density functional incorporates an exchange-correlation functional[26-29] as well as gradient correction[28,29] and a percentage of Hartree-Fock exchange.[30] This method has been used in numerous applications (see Sousa, et al., 2007 for a review) and has been tested in the determination of chemical kinetic quantities.[19,20,31-36]

The ability for Al to readily change its coordination state as discussed above as well as the likelihood of a pentavalent Si intermediate mandates the use of a basis set which includes d orbitals. The 6-311+G(d,p) basis set[37,38] was chosen because it accommodates the d orbitals for Si and Al species, and p orbitals for H were also necessary in the case that H is a reacting constituent in a given reaction. The combination of the B3LYP functional with the 6-311+G(d,p) basis set is employed to determine the mechanism of each reaction in the dissolution of an aluminosilicate mineral.

Ab-initio calculations were performed on each of the clusters and molecules given in Eq. 1–6 using the Gaussian 03 package.[39] Species along the reaction coordinate were optimized at the B3LYP/6-311+G(d,p) level, and transition state structures are characterized by a single negative frequency corresponding to either the formation of a bond between the incoming water and the reacting center or to the breaking of the bond between the reacting center and the O_{br} for the first and second transition states,

respectively. Any deviations from these characteristics are outlined in Sections 3.4.1 and 3.4.2, and each depiction of a reaction mechanism was made with GaussView 4.[40]

The B3LYP functional was chosen for its extensive use in the literature (see Sousa, et al., 2007 for a review) as well as its computational feasibility. However, the B3LYP functional is not necessarily appropriate for every application,[30] and therefore, two other computational methods were tested. The first, PBE1PBE, is a generalized gradient approximation (GGA) type functional[41,42] which builds upon the Perdew-Wang 1991 (PW-91)[43] functional but blends local spin density (LSD) elements with functions of the gradient approximation which are most energetically relevant.[41] In addition, the functional is simplistic in its description of the electron density by replacing all but the LSD with constants[41] as well as the use of one coefficient to control the Hartree-Fock/Density Functional exchange ratio.[42] This method has been tested in the determination of kinetic quantities[44] and has shown strength in the determination of thermokinetic properties of Al materials.[20,45]

The second, M05-2X, is a hybrid meta exchange-correlation functional[19] derived from the M05 functional,[46] and like other functionals in its class, the M05-2X functional adds a kinetic energy component to the exchange-correlation function.[19,46] The aim of the development of the M05 ancestor of the M05-2X functional was to be applicable to a general type of chemical system or process,[46] and the incorporation of two times the nonlocal exchange (2X) is designed to be geared toward analysis of non-metals.[19] In particular, its training function included a parameter regarding its performance with barrier heights,[46] and recently, the M05-2X functional was the strongest choice for

kinetics applications of nonmetal systems among the more popular density functionals used today.[19]

In an effort to study the effects of basis sets on the barrier heights for the reactions presented here, a second basis set was used with each computational method to calculate the barrier height of each reaction. The MG3S basis set includes the 6-311++G(2df,2p) basis set for oxygen, the 6-311+G(3d2f) basis set for aluminum and silicon, and the 6-311+G(2df,2p) basis set for hydrogen[47] and has been used to model the dissolution of quartz.[8] Its ability to calculate barrier heights for aluminosilicate systems as well as its computational intensity will be tested here.

The alternative methods were used to optimize the stationary points on each reaction profile which correspond to the rate limiting step. The energies reported here for comparison are meant to show how each method performs with the same structures, and therefore, differences in the energy values show the capability of each method to study aluminosilicate systems. The relative computation times for each method were taken from calculations where the optimized B3LYP/6-311+G(d,p) transition state from the rate determining step was used as the input geometry, and all calculations were run on the same AMD Opteron Processors.[48] In addition, the relative computation times are included to show how strenuous calculations are with each of these methods, and optimum methods were chosen after consideration of both performance and computational intensity.

3.3 Results

3.3.1 Dissolution Reactions at Si-O_{br}-Al Sites

The reaction profiles for the dissolution reaction for Si-O_{br}-Al sites in the three protonation states are shown in Fig. 4. For the purpose of comparison, dissolution profiles of Si-O_{br}-Si are also included. These profiles show that Si-O_{br}-Al sites proceed through mechanisms with the same number of steps as Si-O_{br}-Si sites for all three protonation states. Protonated sites proceed through a two-step mechanism where the first step is rate limiting, and the barrier heights are nearly identical, 63 and 69 kJ/mol, for Si-O_{br}-Al and Si-O_{br}-Si respectively. Similarly, the neutral site reactions are both one-step processes for Si-O_{br}-Al and Si-O_{br}-Si, and the barrier heights for these reactions are 146 and 159 kJ/mol, respectively. There does appear to be a difference for the deprotonated site reactions, however. The rate limiting step for Si-O_{br}-Al is the second step with a barrier height of 79 kJ/mol, but for Si-O_{br}-Si it is the first step in the dissolution reaction with a barrier height of 110 kJ/mol. The details of these mechanisms for each of these reactions are explained below.

The mechanism for the dissolution of protonated Si sites is shown in Fig. 5 where the Si-O_{br}-Al mechanism appears in the top row, and the Si-O_{br}-Si mechanism is in the bottom row. The mechanisms for Si-O_{br}-Si have appeared previously,[8] but here the previous mechanisms are compared to those for the hydrolysis of Si-O_{br}-Al sites. For the dissolution of Si-O_{br}-Al, the water molecule approaches the Si atom, and a trigonal bipyramidal geometry begins to form around the Si in the TS 1 in Fig. 5. This geometric accommodation allows the H_2O to bond in an axial position in the intermediate (INT), leading to a pentavalent Si species. The TS 2 is a late one where the Si-O_{br} bond is

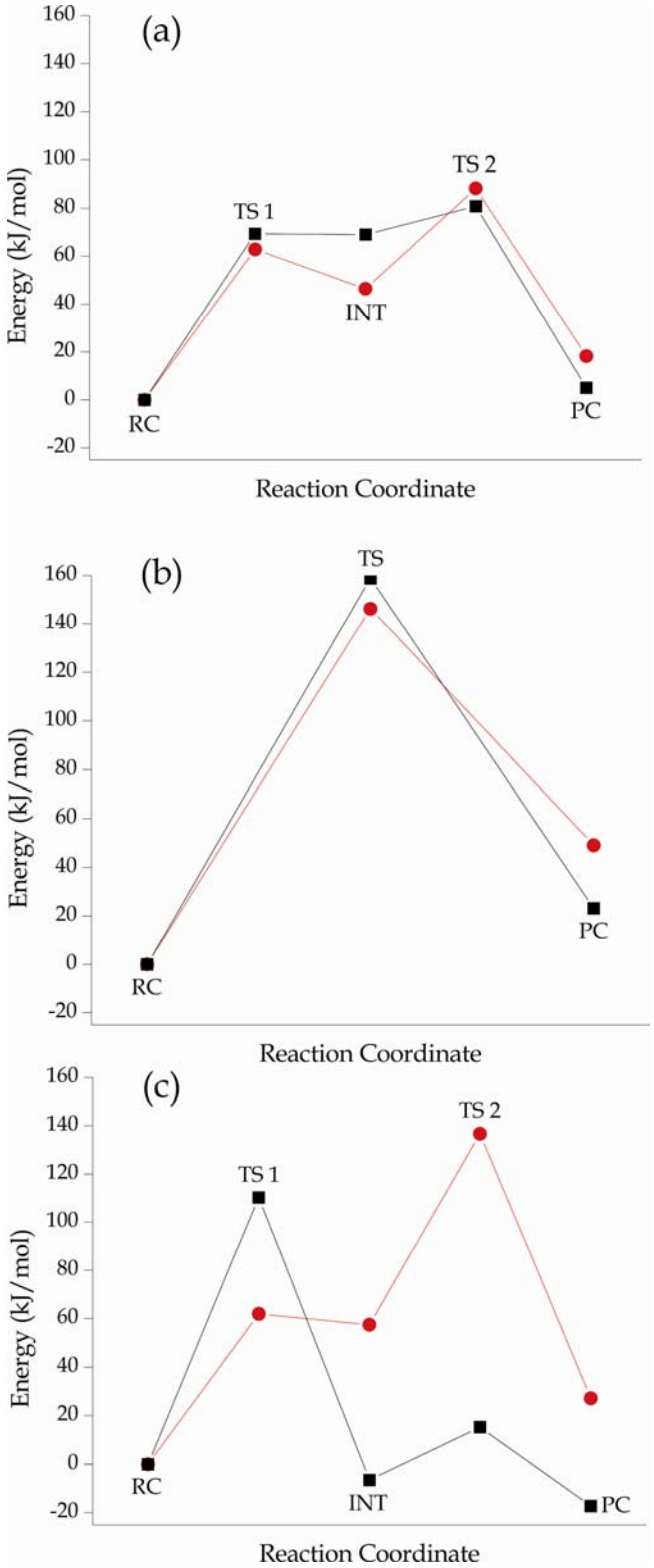

Figure 4: Reaction profiles for sites where Si is the reacting center. Si-O_{br}-Al sites are in red, and Si-O_{br}-Si sites[8] are in black. (a) Protonated. (b) Neutral. (c) Deprotonated.

already broken. Finally, a H^+ transfers to an OH group on the Al atom, leaving both species neutral. The silicon atom has begun to assume a tetrahedral geometry in the TS 2, and that geometry is fully realized in the products of the reaction which are silicic acid and a protonated Al surface site, represented by $[Al(OH)_3(H_2O)]$.

Unlike the protonated site reaction, the neutral site reaction proceeds through a one step mechanism, and the Si-O_{br}-Al and Si-O_{br}-Si mechanisms appear in Fig. 6. For Si-O_{br}-Al, the water approaches the silicon center to what would be an equatorial position if a full trigonal bipyramidal geometry were to result. For Si-O_{br}-Si, on the other hand, the water molecule approaches the Si and bonds in an equatorial position forming a pentavalent transition state. In the dissolution mechanism for Si-O_{br}-Al, the TS is marked by the transfer of H^+ to O_{br} and not by a pentavalent Si state, strictly speaking. However, the TS of this reaction is early, and so the Si-O bond has not yet begun to form. In addition, the Si-O_{br} bond has begun to lengthen in the TS but has not yet broken. Therefore, although the negative frequency described here does not correspond to Si-O bond formation or Si-O_{br} bond break, it is clear that the H^+ transfer to O_{br} is having an effect on these processes. The products here are similar to the protonated reaction except that here silicic acid is released to solution, and the surface remains hydroxylated in the form of $Al(OH)_4^-$.

The dissolution reactions for deprotonated Si-O_{br}-Al and Si-O_{br}-Si sites proceed through a fundamentally similar two step mechanism, and they are shown in Fig. 7. For both reactions, a pentavalent Si species is formed, and then the breaking of the Si-O_{br} bond causes the release of silicic acid into solution. In the reaction for Si-O_{br}-Al, the initially deprotonated O atom in the cluster attracts a H^+ from the incoming water

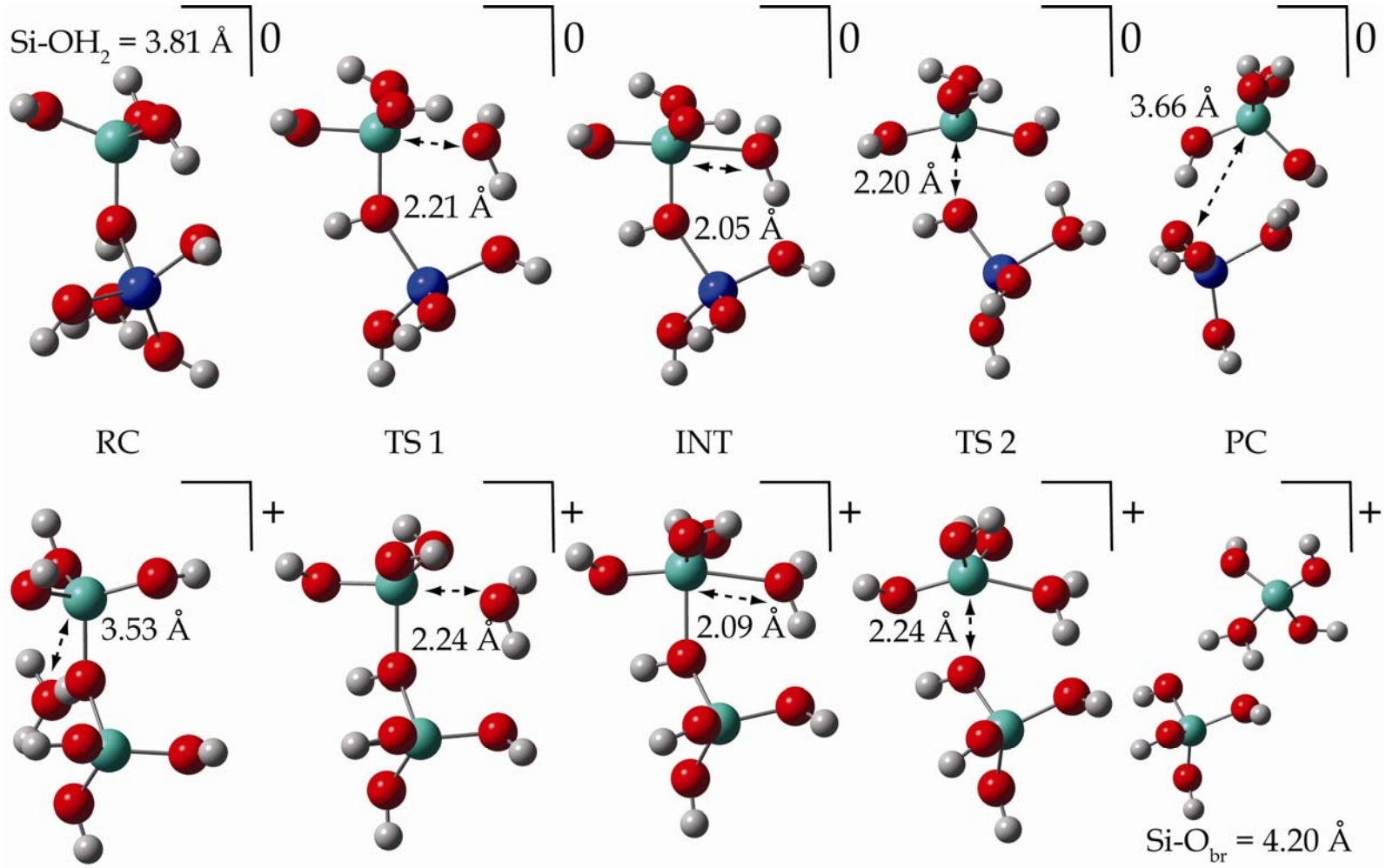

Figure 5: Structures along the reaction profile for protonated sites where Si is the reacting center. Si atoms are shown in cyan, Al atoms in blue, O atoms in red, and H atoms in white. The Si-O_{br}-Al reaction appears in the top row, and the Si-O_{br}-Si reaction[8] appears in the bottom row. RC: reactant complex, TS 1: first transition state, INT: intermediate, TS 2: second transition state, and PC: product complex.

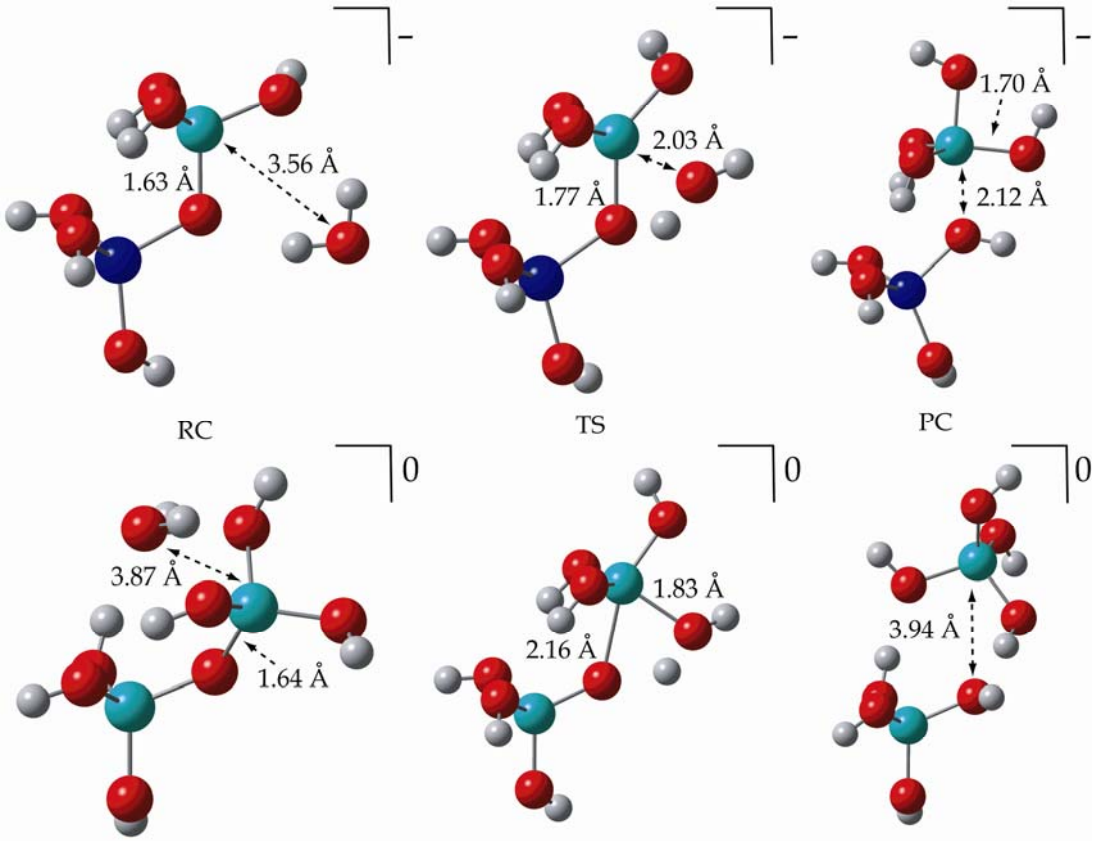

Figure 6: Structures along the reaction profile for neutral sites where the reacting center is Si. Color scheme and structure labeling are the same as Figure 5. Si-O_{br}-Al appears on the top row and Si-O_{br}-Si along the bottom.[8]

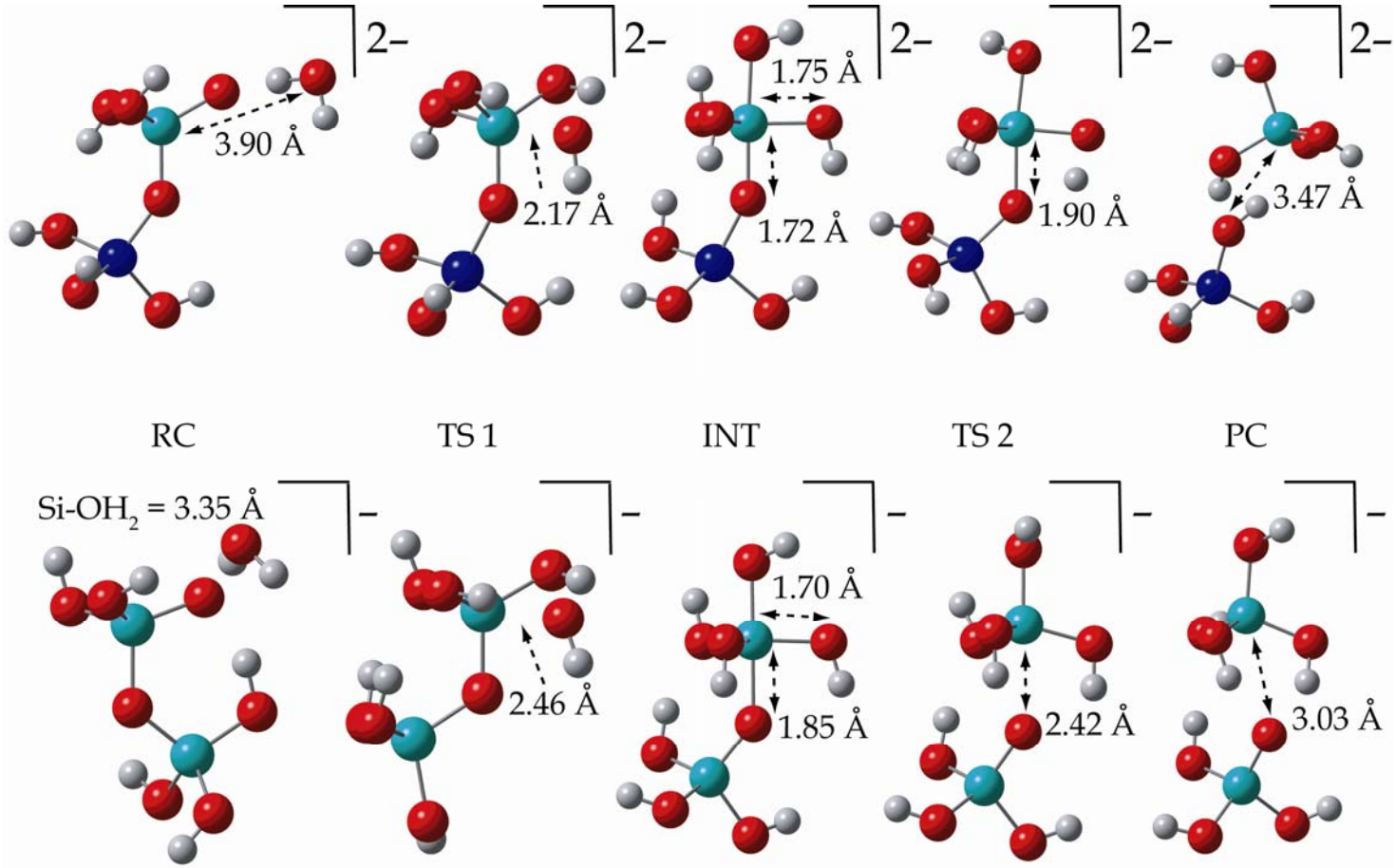

Figure 7: Reaction mechanisms for deprotonated sites where Si is the reacting center. Color scheme and structure labeling are the same as Figure 5, and Si-O_{br}-Al sites are in the top row with Si-O_{br}-Si^8 in the bottom as before.

molecule causing the OH bond to elongate. Once the H^+ has attached to the deprotonated O atom, the remaining OH^- attacks the Si center at an equatorial position, and the bond is fully formed in the INT. The breaking of the Si-O_{br} bond is a concerted motion which involves the transfer of a H^+ to the O_{br} as the Si-O_{br} bond is breaking. In the TS 2, the Si-O_{br} bond is intact but elongated, and the H^+ has already begun to migrate toward O_{br}. A deprotonated silicic acid, $Si(OH)_3O^-$, is released to solution, and the $Al(OH)_4^-$ represents a hydroxylated surface.

Detailed analyses regarding the similarities and differences of Si-O_{br}-Al sites with Si-O_{br}-Si sites as well as a comparison to additional literature are included in the Discussion section.

3.3.2 Dissolution Reactions at Al-O_{br}-Si Sites

In this section, the focus is the dissolution reactions for Al-O_{br}-Si sites as protonated, neutral, and deprotonated. The energy profiles for dissolution reactions at Al-O_{br}-Si sites appear in Fig. 8, and although the scale for the reaction energy is the same as in Fig. 4, the barrier heights are much smaller for the protonated and neutral Al-O_{br}-Si sites. Each site proceeds through a one step mechanism, and the barrier heights are 38, 39, and 79 kJ/mol, respectively. The reactions all include the approach of water to the Al center and the breaking of the Al-O_{br} bond, but the specific process of each mechanism is different. Each mechanism is depicted in Figs. 9–11 and will be described below.

For protonated sites Al-O_{br}-Si sites, the dissolution reaction proceeds through a one step mechanism which is shown in Fig. 9. The bulkiness and the number of groups surrounding the Al atom makes the initial approach of the water molecule sterically

difficult. The H-bonding network that develops stabilizes the secondary water even though it is the seventh group to surround Al. The breaking of the Al-O_{br} bond in the TS in Fig. 9 leaves the Al in a square pyramidal geometry because the distance between Al and the O_{br} is too small to allow rearrangement into a trigonal bipyramidal or other type of geometry, and therefore, addition of the water to the Al atom in the TS is not possible. After the Al-O_{br} distance has increased to a sufficient degree, the Al atom absorbs the secondary water to form $Al(H_2O)_6^{3+}$ in an essentially barrierless step, and the surface remains hydroxylated. The product complex of this reaction is comprised of $Al(H_2O)_6^{3+}$ and a hydroxylated surface represented by $Si(OH)_4$ and is depicted in Fig. 9, and in the product complex, the $Al(H_2O)_6^{3+}$ assumes an orientation to maximize its H-bonding capabilities.

To simulate the existence of a neutral Al-O_{br}-Si site, an aluminosilicate cluster with four water molecules and the silicic acid group around Al was reacted with a water molecule. The initially penta-coordinated Al absorbs the secondary water before the start of the reaction to assume the optimal octahedral Al configuration as the reactant complex (RC) shown in Fig. 10. In addition, the O_{br} was protonated because penta-coordinated Al exists from slightly acidic to neutral pH.[10,11] The mechanism for the dissolution of a neutral Al-O_{br}-Si site is a one step reaction and is shown in Fig. 10 where the incoming water molecule is circled red. The tendency of Al to readily change its coordination state[10,11] is reinforced in the transition state for this reaction which shows that the Al-O_{br} bond has already broken and that the incoming water molecule has migrated from the

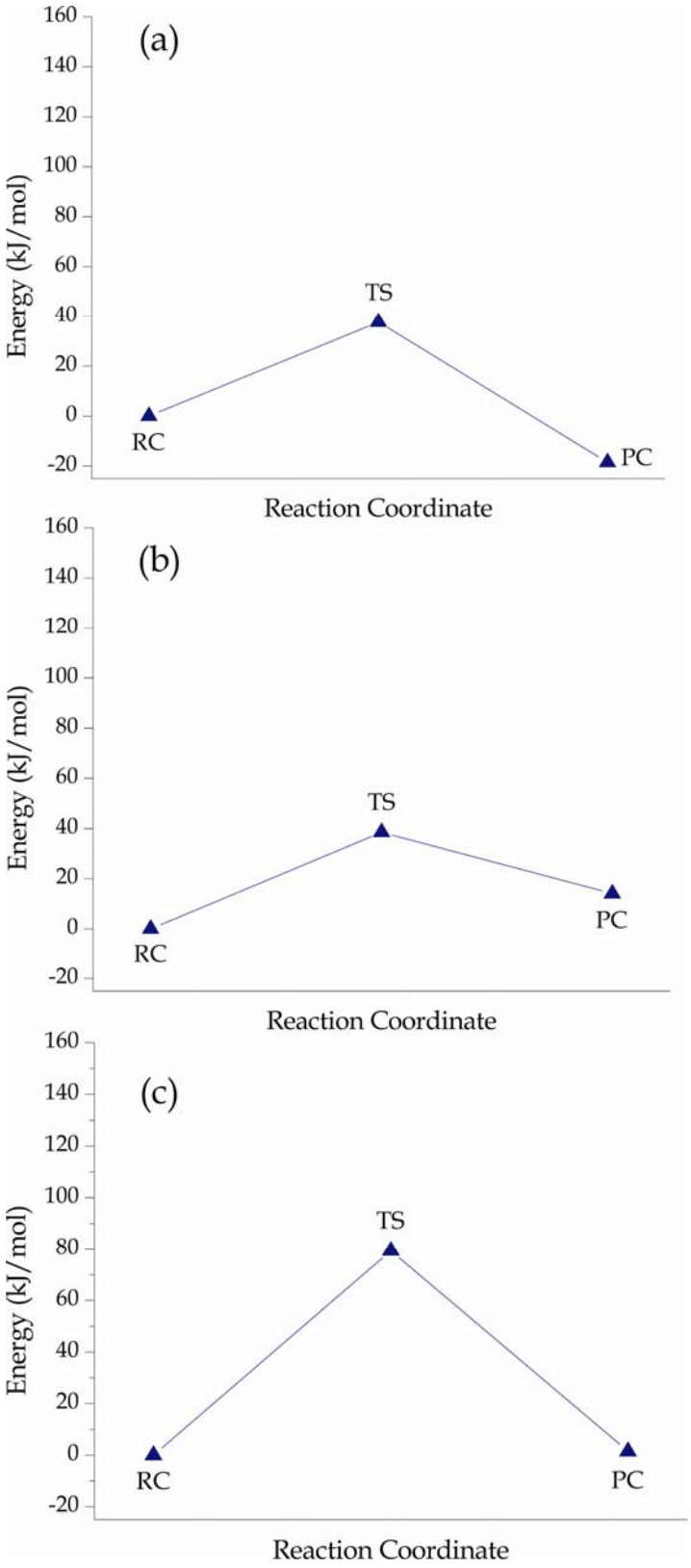

Figure 8: Reaction profiles for dissolution reactions at the Al-O_{br}-Si sites. (a) Protonated. (b) Neutral. (c) Deprotonated.

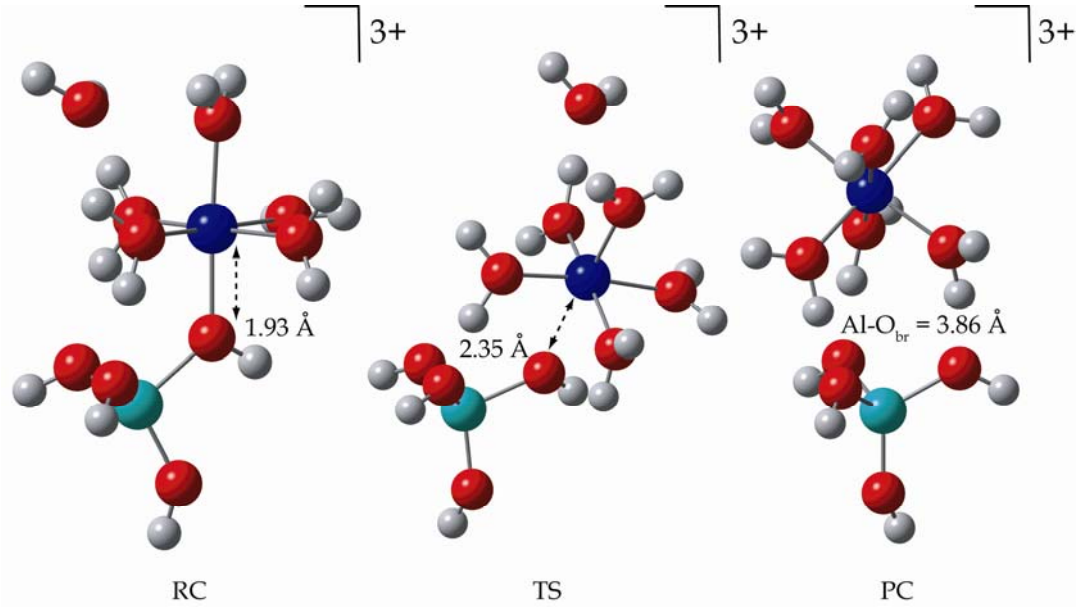

Figure 9: Reaction mechanism for protonated Al-O_{br}-Si sites. Color scheme and structure labeling are the same as Figure 5.

primary to the secondary hydration shell. When the Al-O_{br} bond has fully broken in the product complex, shown in Fig. 10, H_3O^+, $[Al(OH)_2(H_2O)_2]^+$, and a protonated surface, $[Si(OH)_3(H_2O)]^+$, remain, and the Al atom has fully formed into a tetrahedral geometry. There is also an extensive hydrogen bonding network occurring in the PC between water and OH groups on the Al and Si atoms as well as between the H_3O^+ and a OH group on the Al atom. This H-bonding prevents the hydronium ion constituents from being reabsorbed by the Al atom. This reaction proceeds through a dissociative interchange mechanism in that there are two bonds breaking simultaneously, and there is a possibility for increased coordination for the product species which would exist in water.[49]

The dissolution reaction for deprotonated Al-O_{br}-Si sites follows the logic that Al is tetra-coordinated in basic media,[10,11] and the mechanism for this reaction appears in Fig. 11. The water molecule approaches the Al atom in an equatorial approach if a trigonal bipyramidal geometry were fully realized, and the transition state is a late one where the Al-O_{br} bond is already broken. The transition state is marked by the breaking of the Al-O_{br} bond, and the H^+ from the incoming water molecule has already transferred to the O_{br}. The H^+ transfer to the O_{br} is necessary to keep the single negative charge on the Al species, and the continuation of a tetrahedral geometry around the Al atom is evident. This leaves the surface hydroxylated, and $Al(OH)_4^-$ is released to solution.

An analysis of Al-O_{br}-Si sites for all three protonation states as well as a comparison to previous ab-initio calculations follow in the Discussion section.

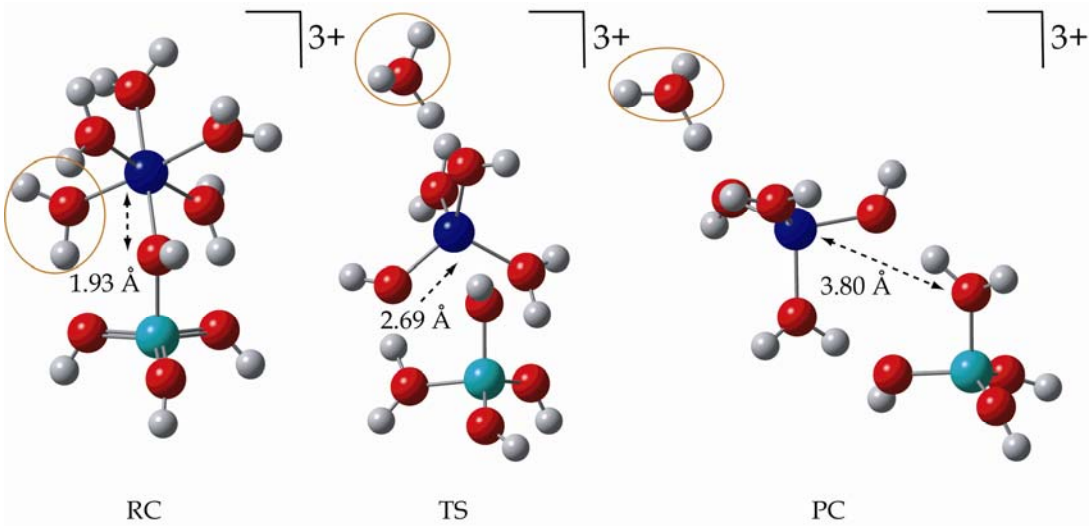

Figure 10: Reaction mechanism for neutral Al-O_{br}-Si sites. Color scheme and structure labeling are the same as Figure 5. The red circle shows the incoming water which is initially absorbed then is released to solution as Al changes its coordination.

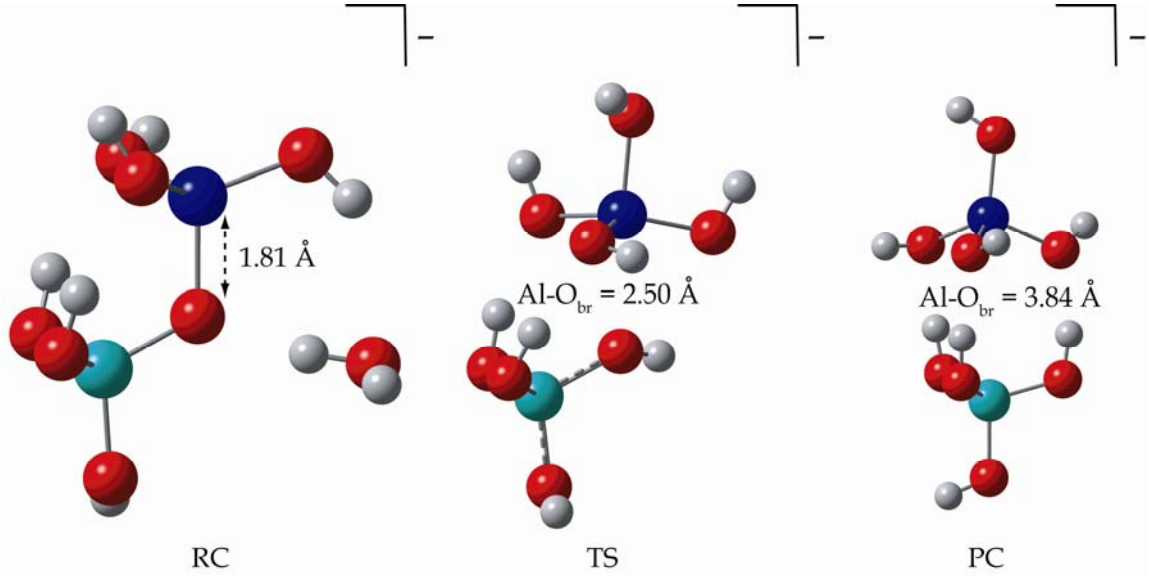

Figure 11: Reaction mechanism for deprotonated Al-O$_{br}$-Si sites. Color scheme and structure labeling are the same as Figure 5.

3.3.3 Comparison of Alternative Methods

The aim of using the PBE1PBE and M05-2X functionals as well as the MG3S basis set is to determine whether these computational methods show the same trends shown above with the B3LYP/6-311+G(d,p) calculations for the model of aluminosilicate dissolution studied here. The barrier heights for the rate limiting steps in each of the dissolution reactions for Si-O_{br}-Al and Al-O_{br}-Si sites are presented in Table 1. The averages correspond to the arithmetic mean of the barrier heights calculated for all the methods, and the standard deviation (σ) includes all six barrier heights as well. The table is arranged such that basis set calculations with the same functional are grouped together, and barrier height values which are outside the bounds of the average and standard deviation values are underlined for each reaction.

The barrier heights in Table 1 for Si-O_{br}-Al sites replicate the same trends. That is, the neutral Si-O_{br}-Al sites always have the greatest barrier height, then the deprotonated, and the protonated sites have the lowest barrier heights. The range of the standard deviation around the average shows that the barrier height values do not overlap for Si-O_{br}-Al sites. In addition, barrier heights calculated with the MG3S basis set are always higher than those with 6-311+G(d,p). The inclusion of diffuse functions on non-hydrogen atoms has been shown to decrease the error associated with calculations using smaller basis sets, but each of these basis sets has the same number of diffuse functions for all but the hydrogen atoms.[47] Thus the reason for this increase is not immediately clear.

Table 1: Barrier heights (kJ/mol) for the rate limiting step in each reaction using B3LYP, PBE1PBE, and M05-2X functionals with 6-311+G(d,p) and MG3S basis sets. The underlined values are those which lie outside the range of the mean and standard deviation values.

Reacting Center	Type of Site	B3LYP		PBE1PBE		M05-2X		Average	Standard Deviation
		6-311+G(d,p)	MG3S	6-311+G(d,p)	MG3S	6-311+G(d,p)	MG3S		
Si	Protonated	<u>63</u>	58	49	54	<u>45</u>	48	53	7
	Neutral	146	<u>166</u>	<u>133</u>	155	152	161	152	12
	Deprotonated	<u>79</u>	83	<u>79</u>	85	85	<u>90</u>	84	4
Al	Protonated	<u>38</u>	<u>58</u>	42	44	49	50	47	7
	Neutral	39	35	52	35	<u>73</u>	54	48	15
	Deprotonated	79	88	81	<u>92</u>	79	89	85	6

For Al-O_{br}-Si sites, the deprotonated barrier height is always the highest, but the lowest value is either the neutral or the protonated site for each functional or basis set. Thus no overall trend exists among the methods chosen. The largest standard deviation among all Si-O_{br}-Al and Al-O_{br}-Si sites is among the barrier heights for neutral Al-O_{br}-Si sites. One possibility is that this reaction is the only unimolecular decomposition, but a previous study found comparable performance of these methods in calculating the barrier heights of unimolecular reactions as well as other types of reactions.[33]

The relative computation times in minutes for each method are compiled in Table 2, and the MG3S basis set requires more computation time than the 6-311+G(d,p) basis set. Generally speaking, the PBE1PBE functional requires the least computation time for each of the three functionals tested, and the next most feasible functional alternates between B3LYP and M05-2X for the Si-O_{br}-Al and Al-O_{br}-Si sites in all three protonation states.

PBE1PBE functional requires the least amount of computation time. For calculations with the 6-311+G(d,p) basis set, B3LYP is the next least computationally demanding functional, while for the MG3S basis set, the M05-2X follows PBE1PBE in computational intensity. However, the greatest increase in computation time comes from changing the basis set from 6-311+G(d,p) to MG3S, and this is true for every functional.

Table 2: Computation time (min) for B3LYP, PBE1PBE, and M05-2X methods using 6-311+G(d,p) and MG3S basis sets to calculate the barrier height for each dissolution reaction.

Reacting Center	Type of Site	B3LYP		PBE1PBE		M05-2X	
		6-311+G(d,p)	MG3S	6-311+G(d,p)	MG3S	6-311+G(d,p)	MG3S
Si	Protonated	6	40	3	13	8	45
	Neutral	6	44	3	13	7	40
	Deprotonated	9	56	5	21	6	40
Al	Protonated	15	75	11	77	17	92
	Neutral	8	48	5	19	12	69
	Deprotonated	5	37	6	39	8	42

3.4 Discussion

3.4.1 Trends for Si-O_{br}-Si, Si-O_{br}-Al, and Al-O_{br}-Si and Comparison to Experiment

The barrier heights for the dissolution reactions for protonated and neutral Al-O_{br}-Si sites are much lower than those for either Si-O_{br}-Si or Si-O_{br}-Al sites. In addition, the dissolution mechanisms for Si-O_{br}-Si and Si-O_{br}-Al sites are nearly identical. Both sets of reactions proceed through the same number of steps and have similar barrier heights for protonated, neutral, and deprotonated sites. The Al-O_{br}-Si sites proceed through dissolution mechanisms that are independent of one another and do not resemble the dissolution for Si-O_{br}-Al sites.

The dissolution reactions for Al-O_{br}-Si sites are similar in that they are all one-step processes as shown in the energy profiles in Fig. 8, but the mechanisms depicted in Figs. 9–11 demonstrate that each reaction proceeds quite differently. The protonated Al-O_{br}-Si sites show a decrease in coordination around the Al atom only to return to an octahedral configuration in the product complex. The neutral sites, on the other hand, do not reabsorb the secondary water molecule in the product complex. Lastly, the barrier height in the dissolution reaction for deprotonated Al-O_{br}-Si sites corresponds to the Al-O_{br} bond break and is much higher than for protonated and neutral sites, and the tetrahedral geometry around the Al atom is maintained throughout the reaction.

The barrier heights calculated here as well as those for Si-O_{br}-Si sites[8] and protonated and neutral Al-O_{br}-Si sites[22] are given in Table 3. The barrier heights decrease in the order Si-O_{br}-Si, Si-O_{br}-Al, and the Al-O_{br}-Si data from this work which mimics experiment in that Al leaches out before Si in low to neutral pH ranges[15,16] and

that the dissolution rate is at a minimum under neutral pH conditions but increases in both acidic and basic pH ranges.[1]

The difference between the barrier heights from Xiao and Lasaga[22] and those presented here warrants additional comment. For the protonated and neutral Al-O_{br}-Si sites, Xiao and Lasaga placed the water molecule in their study directly between the Al and Si centers, while here the water molecule was maintained closer to one center or the other to enable determination of the barrier height for each type of dissolution reaction. In addition, the clusters used in the dissolution reactions studied here are likely more representative in their incorporation of various Al coordination states, while the Al-O_{br}-Si model cluster used by Xiao and Lasaga included a tetra-coordinated Al atom.

A collection of experimental activation energy (E_a) values for albite[50-52] appears in Table 4. One challenge of comparing the barrier heights calculated here to experimental E_a values is that the E_a values from experiment include Si-O_{br}-Si, Si-O_{br}-Al, and Al-O_{br}-Si sites in all protonation states. Thus they are an average over the whole surface, and a direct comparison would require knowledge of how many of each site exists on the surface and in which protonation state. Although the E_a values from Table 4 are lower than those for Si-O_{br}-Si and Si-O_{br}-Al, this may be an indication that the contribution of low barrier heights from the dissolution of Al-O_{br}-Si sites aids in the overall dissolution of aluminosilicate minerals.

Table 3: Ab-initio barrier heights (kJ/mol) for protonated, neutral, and deprotonated sites for Si-O_{br}-Si calculated with B3LYP/6-31+G(d,p),[8] Si-O_{br}-Al and Al-O_{br}-Si from this work, and protonated and neutral Al-O_{br}-Si sites using MP2/6-31G(d).[22]

Type of Site	Protonated	Neutral	Deprotonated
Si-O_{br}-Al	63	146	79
Al-O_{br}-Si	38	39	79
Si-O_{br}-Si [8]	69	159	110
Al-O_{br}-Si [22]	67	109	NA

Table 4: Experimental activation energy (E_a) values (kJ/mol) for the dissolution of albite at various pH ranges.[50-52]

pH	Blum and Stillings	Chen and Brantley	Hellmann
Acidic	60.0	65.3	88.9 ± 14.6
Neutral	67.7	NA	68.8 ± 4.5
Basic	50.1	NA	85.2

3.4.2 Comparison of Si-O_{br}-Al Sites with Si-O_{br}-Si Sites

In total, the dissolution reactions for Si-O_{br}-X, where X is either Si or Al, are fundamentally identical. For protonated, neutral, and deprotonated sites, the Si-O_{br}-Al dissolution reactions proceed through mechanisms in much the same way as their Si-O_{br}-Si counterparts, and their associated barrier heights are comparable. For the protonated and neutral sites, the barrier height corresponds to the water approaching the Si center. When comparing the Si-O_{br}-Si and Si-O_{br}-Al reactions for deprotonated sites, the barrier heights correspond to two different steps. In the reaction for Si-O_{br}-Si, the rate limiting step is the formation of the pentavalent Si intermediate, while for Si-O_{br}-Al, the rate limiting step is the breaking of the Si-O_{br} bond. In addition, the barrier heights for Si-O_{br}-Al sites are lower than for Si-O_{br}-Si which would allow Si species from these sites to be released to solution before those from Si-O_{br}-Si sites.

In the dissolution reaction for protonated sites where Si-O_{br}-Al and Si-O_{br}-Si sites are hydrolyzing, the mechanisms proceed through two steps[8] shown in Fig. 5. One can see that protonated site dissolution reactions proceed in the same fashion when the Si-O_{br} bond breaks, regardless of whether Si or Al is the non-reacting atom. Both reactions proceed through a two step mechanism where the formation of a pentavalent Si precedes the breaking of the Si-O_{br} bond, and the rate determining step in each reaction is the formation of the Si-O bond leaving Si in a pentavalent state.

There are, however, some slight differences between the product species for the two reactions. For the Si-O_{br}-Si reaction, the positively charged species is released to solution while for the Si-O_{br}-Al system, the surface remains protonated. For this aluminosilicate model system, the transfer of H^+ to the OH group on the Al atom can be

expected because otherwise the silicic acid species would be protonated, and the Al species would hold a negative charge. Therefore the H^+ transfer enables the formation of two neutral species. Further, the acid dissociation constant is higher for silicic acid than aqueous aluminum species.[10,53]

In the neutral sites reaction for Si-O_{br}-Al, the transition state corresponds to the transfer of a H^+, while for Si-O_{br}-Si the transition state corresponds to the formation of a pentavalent Si. Although attempts to isolate a pentavalent Si for Si-O_{br}-Al were unsuccessful, the barrier heights for these two systems are comparable. However, experimental findings did not show a kinetic isotope effect for silicate dissolution[54] which would indicate that a H^+ transfer is not likely to occur during dissolution. Additional analysis into this dissolution reaction mechanism may be warranted.

Although the dissolution reactions for Si-O_{br}-Si and Si-O_{br}-Al deprotonated sites proceed through a similar fashion, the reaction profiles, shown in Fig. 4, demonstrate some differences for these two reactions. For Si-O_{br}-Si, the rate limiting step is the formation of the pentavalent intermediate, while for Si-O_{br}-Al, the rate determining step for this reaction is the breaking of the Si-O_{br} bond. In addition, the intermediate for Si-O_{br}-Al is a cluster with a greater negative charge than that for Si-O_{br}-Si, and the localization of that charge throughout a small volume causes the intermediate to be higher in energy for the Si-O_{br}-Al dissolution reaction. Then this species dissociates into two clusters each with a (–1) charge which leads to repulsion of the two species in the product complex for Si-O_{br}-Al that is not present in the Si-O_{br}-Si reaction.

3.4.3 Analysis of Al-O_{br}-Si Sites and Comparison to Literature

To summarize, Al-O_{br}-Si sites proceed in a much different fashion from Si-O_{br}-Al and Si-O_{br}-Si sites and also very differently from one another. The main reason for this difference is that the representative sites do not differ by merely a H^+ as with Si-O_{br}-Al or Si-O_{br}-Si sites. However, the barrier heights for the Al-O_{br}-Si reactions are quite similar for protonated and neutral sites. For both the protonated and neutral sites, the one step mechanism is characterized by the breakage of the Al-O_{br} bond and a decrease of Al coordination in the transition state. For the protonated site, this decrease allows for the addition of the secondary water, but in the neutral site reaction, the H-bonding network prevents the immediate addition of the water to the Al atom. For the deprotonated site, the equatorial attack of the incoming water molecule simultaneously weakens the Al-O_{br} bond and allows for the transfer of H^+ to the O_{br}, resulting in a late transition state.

The initial attempts to locate a transition state for the protonated Al-O_{br}-Si dissolution reaction included a *cis* approach of the incoming water molecule and a heptavalent Al center, but the *trans* approach of the water molecule was successful. The *cis* and *trans* approaches of an incoming water molecule[21] toward the cluster representing the protonated Al-O_{br}-Si sites are pictured in Fig. 12 and are two possibilities for the path of this reaction. These two approaches were modeled in a recent description by Evans, et al. of water exchange reaction mechanisms on a hexaaqua Al ion.[21] Their calculations showed that the *cis* approach of a water molecule was a lower energy process than the *trans*. However, their *trans* transition state had two negative frequencies, and MD calculations show the *trans* approach to be the more prevalent reaction process.[21] Our calculations show the *trans* approach to be lower in energy by

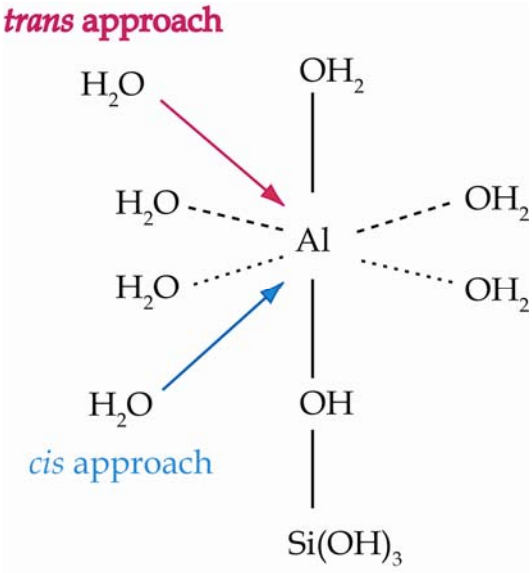

Figure 12: Schematic of *cis* and *trans* approaches of a water molecule[21] to a protonated Al-O_{br}-Si site.

more than 40 kJ/mol (data not shown), and in particular, the *cis* approach would be a higher energy process due to steric hindrance from the silicic acid group.

The hepta-coordinated Al in the transition state initially seemed logical because Al can accommodate four, five, or six groups in stable species. However when the secondary water was added to an equatorial position around the Al, this structure did not result in a stable geometry. Although it is possible for larger metals to interact through a hepta-coordinated state, Al does not behave in this manner.[55] The isolation of a single frequency transition state for the *trans* approach for water toward an Al center with a reasonable barrier height as well as previous studies of the *cis* approach of water[21] and hepta-coordinated Al ion[55] give confidence to the reaction mechanism for the protonated Al-O_{br}-Si site described here.

The neutral Al-O_{br}-Si site dissolution reaction mechanism could at first glance seem unreasonable. The incoming water is at first absorbed, and the Al-O bonds connecting it and the $Si(OH)_4$ group to Al simultaneously break. This type of dissolution reinforces the propensity of Al to readily change its coordination state,[10,11] and a decrease in coordination as well as the formation of H_3O^+ has been seen in water exchange reactions with the hexaaqua Al ion.[21] In fact, Evans, et al.[21] constrained the geometries of their reacting species to prevent such an occurrence. Furthermore, the presence of this reaction in the solution phase would enable surrounding water molecules to easily be absorbed by Al leading to the optimal hexa-coordinated Al. The reaction description given here is meant to show the process by which the Al species is released to solution from a neutral site.

The tetra-coordinated Al-O_{br}-Si site does not behave similarly to either of the other two Al-O_{br}-Si sites in that there is no decrease in coordination. Instead, the water molecule is absorbed by Al, and a H^+ is transferred to an OH group on Si. However, the reason for the much larger barrier height for this reaction is not clear. Nonetheless, the dissolution experiments performed by Hamilton, et al. did not show Al leaching first from aluminosilicate minerals at basic pH,[6] where a significant number of deprotonated sites is likely to exist,[9] and the higher barrier height for deprotonated Al-O_{br}-Si sites could be an explanation for this observation.

3.4.4 Role of Charge in the Dissolution Mechanism

In aluminosilicate minerals, charge-balancing cations leach out first, leaving behind Al and Si constituents.[15,16] Therefore, an analysis of the dissolution reaction mechanisms can exclude a charge-balancing cation. Further, the aim of this work is to examine how the reactions proceed and to calculate the barrier height of each reaction in an effort to shed light on the dissolution of aluminosilicate minerals and how each species is released to solution.

Two observations concerning the role of charge in these reactions can be delineated. The first is that the addition of a H^+ to each reaction as one moves from deprotonated to neutral to protonated sites clearly has an effect for Si-O_{br}-Al because the mechanisms and barrier heights are different for each type of site. In addition, early calculations of the deprotonated Al-O_{br}-Si site showed a completely different, two step mechanism when OH^- was reacted with the cluster instead of H_2O (data not shown). On the other hand, the Si-O_{br}-Si and Si-O_{br}-Al mechanisms and barrier heights are nearly

identical to one another even though the charges of each respective site are different from one another. Furthermore, the protonated and neutral Al-O_{br}-Si sites have the same overall charge (+3), but the addition of one H_2O changes the mechanism drastically. Thus it seems that both chemical constituents as well as overall charge of a system contribute to the reaction mechanism.

3.5 Conclusion

The ab initio calculations presented here show that Al species from protonated and neutral Al-O_{br}-Si sites can leach before Si species, and this trend matches experiment.[1,6] In addition, the Si-O_{br}-Al dissolution mechanisms determined by this work are fundamentally identical to those for Si-O_{br}-Si sites.[8] The barrier heights for the rate limiting steps for each reaction were also calculated with the B3LYP, PBE1PBE, and M05-2X functionals in combination with the 6-311+G(d,p) and MG3S basis sets, and the trends from the B3lYP/6-311+G(d,p) mechanism calculations were repeated. Lastly, single point calculations to determine optimal computational methods showed that any of the B3LYP, PBE1PBE, or M05-2X functionals would be desirable choices for both performance and computation time.

The barrier heights for Si-O_{br}-Al sites calculated with B3LYP/6-311+G(d,p) are 63, 146, and 79 kJ/mol, respectively, and the barrier heights and mechanisms determined here for Si-O_{br}-Al are comparable to those for Si-O_{br}-Si dissolution reactions.[8] For Al-O_{br}-Si sites, the barrier heights are 38, 39, and 79 kJ/mol using B3LYP/6-311+G(d,p) as well. The mechanisms for protonated and neutral sites are similar to water exchange reactions around the hexaaqua Al ion,[21] but the Al-O_{br} bond break for deprotonated

Al-O_{br}-Si sites results in an anomalously high barrier height for reasons unclear at this time.

The mechanisms presented and the barrier heights calculated here mimic trends seen in experiment as well as expectations as to how these dissolution reactions proceed. Ab initio calculations have shown to be useful tools, and any of these functionals is recommended with the 6-311+G(d,p) basis set for determining the barrier heights of reactions involving aluminosilicate materials. Additional study is required to link these barrier heights to dissolution rates seen in the field, but the initial correlation with previous trends shown here is promising.

References

(1) Brantley, S. L. Kinetics of mineral dissolution. In *Kinetics of Water-Rock Interaction*; Brantley, S. L., Kubicki, J. D., White, A. F., Eds.; Springer: New York, NY, 2008; pp 151.

(2) Swaddle, T. W.; Salerno, J.; Tregloan, P. A. *Chemical Society Reviews* **1994**, *23*, 319.

(3) Swaddle, T. W. *Coordination Chemistry Reviews* **2001**, *219*, 665.

(4) Birchall, J. D.; Exley, C.; Chappell, J. S.; Phillips, M. J. *Nature* **1989**, *338*, 146.

(5) Neese, W. D. *Introduction to Mineralogy*; Oxford University Press: New York, NY, 2000.

(6) Hamilton, J. P.; Brantley, S. L.; Pantano, C. G.; Criscenti, L. J.; Kubicki, J. D. *Geochimica et Cosmochimica Acta* **2001**, *65*, 3683.

(7) Tsomaia, N.; Brantley, S. L.; Hamilton, J. P.; Pantano, C. G.; Mueller, K. T. *American Mineralogist* **2003**, *88*, 54.

(8) Nangia, S.; Garrison, B. J. *Journal of Physical Chemistry A* **2008**, *112*, 2027.

(9) Dove, P. M.; Elston, S. F. *Geochimica et Cosmochimica Acta* **1992**, *56*, 4147.

(10) Martin, R. B. *Journal of Inorganic Biochemistry* **1991**, *44*, 141.

(11) Swaddle, T. W.; Rosenqvist, J.; Yu, P.; Bylaska, E.; Phillips, B. L.; Casey, W. H. *Science* **2005**, *308*, 1450.

(12) Knauss, K. G.; Wolery, T. J. *Geochimica et Cosmochimica Acta* **1988**, *52*, 43.

(13) Schwartzentruber, J.; Furst, W.; Renon, H. *Geochimica et Cosmochimica Acta* **1987**, *51*, 1867.

(14) Wollast, R.; Chou, L. In *NATO ASI Series*; Lerman, A., Meybeck, M., Eds.; NATO: Geneva, 1988; Vol. 251; pp 11.

(15) Hellmann, R.; Eggleston, C. M.; Hochella, M. F., Jr.; Crear, D. A. *Geochimica et Cosmochimica Acta* **1990**, *54*, 1267.

(16) Stillings, L. L.; Brantley, S. L. *Geochimica et Cosmochimica Acta* **1995**, *59*, 1483.

(17) Oelkers, E. H.; Schott, J. *Geochimica et Cosmochimica Acta* **1995**, *59*, 5039.

(18) Criscenti, L. J.; Brantley, S. L.; Mueller, K. T.; Tsomaia, N.; Kubicki, J. D. *Geochimica et Cosmochimica Acta* **2005**, *69*, 2205.

(19) Zhao, Y.; Schultz, N. E.; Truhlar, D. G. *Journal of Chemical Theory and Computation* **2006**, *2*, 364.

(20) Schultz, N. E.; Truhlar, D. G. *Journal of Chemical Theory and Computation* **2005**, *1*, 41.

(21) Evans, R. J.; Rustad, J. R.; Casey, W. H. *Journal of Physical Chemistry A* **2008**, *112*, 4125.

(22) Xiao, Y.; Lasaga, A. C. *Geochimica et Cosmochimica Acta* **1994**, *58*, 5379.

(23) Kubicki, J. D. Transition state theory and molecular orbital calculations applied to rates and reaction mechanisms in geochemical kinetics. In *Kinetics of Water-Rock Interaction*; Brantley, S. L., Kubicki, J. D., White, A. F., Eds.; Springer: New York, 2008; pp pg. 39.

(24) Kubicki, J. D.; Blake, G. A.; Apitz, S. E. *American Mineralogist* **1996**, *81*, 789.

(25) Foresman, J. B.; Frisch, A. *Exploring Chemistry with Electronic Structure Methods*, 2nd ed.; Gaussian, Inc.: Pittsburgh, 1996.

(26) Vosko, S. H.; Wilk, L.; Nusair, M. *Canadian Journal of Physics* **1980**, *58*, 1200.

(27) Lee, C.; Yang, W.; Parr, R. G. *Physical Review B* **1988**, *37*, 785.

(28) Becke, A. D. *Journal of Chemical Physics* **1993**, *98*, 1372.

(29) Becke, A. D. *Journal of Chemical Physics* **1993**, *98*, 5648.

(30) Sousa, S. F.; Fernandes, P. A.; Ramos, M. J. *Journal of Physical Chemistry A* **2007**, *111*, 10439.

(31) Andersson, S.; Gruning, M. *Journal of Physical Chemistry A* **2004**, *108*, 7621.

(32) Zhao, Y.; Pu, J.; Lynch, B. J.; Truhlar, D. G. *Physical Chemistry Chemical Physics* **2004**, *6*, 673.

(33) Zhao, Y.; Gonzalez-Garcia, N.; Truhlar, D. G. *Journal of Physical Chemistry A* **2005**, *109*, 2012.

(34) Zhao, Y.; Truhlar, D. G. *Journal of Physical Chemistry A* **2005**, *109*, 5656.

(35) Riley, K. E.; Op't Holt, B. T.; Merz, K. M., Jr. *Journal of Chemical Theory and Computation* **2007**, *3*, 407.

(36) Zheng, J.; Zhao, Y.; Truhlar, D. G. *Journal of Chemical Theory and Computation* **2007**, *3*, 569.

(37) Krishnan, R.; Binkley, J. S.; Seeger, R.; Pople, J. A. *Journal of Chemical Physics* **1980**, *72*, 650.

(38) Clark, T.; Chandrasekhar, J.; Spitznagel, G. W.; von Rague Schleyer, P. *Journal of Computational Chemistry* **1983**, *4*, 294.

(39) Frisch, M. J.; Trucks, G. W.; Schlegel, H. B.; Scuseria, G. E.; Robb, M. A.; Cheeseman, J. R.; Montgomery, J. A., Jr.; Vreven, T.; Kudin, K. N.; Burant, J. C.; Millam, J. M.; Iyengar, S. S.; Tomasi, J.; Barone, V.; Mennucci, B.; Cossi, M.; Scalmani, G.; Rega, N.; Petersson, G. A.; Nakatsuji, H.; Hada, M.; Ehara, M.; Toyota, K.; Fukuda, R.; Hasegawa, J.; Ishida, M.; Nakajima, T.; Honda, Y.; Kitao, O.; Nakai, H.; Klene, M.; Li, X.; Knox, J. E.; Hratchian, H. P.; Cross, J. B.; Bakken, V.; Adamo, C.; Jaramillo, J.; Gomperts, R.; Stratmann, R. E.; Yazyev, O.; Austin, A. J.; Cammi, R.; Pomelli, C.; Ochterski, J. W.; Ayala, P. Y.; Morokuma, K.; Voth, G. A.; Salvador, P.; Dannenberg, J. J.; Zakrzewski, V. G.; Dapprich, S.; Daniels, A. D.; Strain, M. C.; Farkas, O.; Malick, D. K.; Rabuck, A. D.; Raghavachari, K.; Foresman, J. B.; Ortiz, J. V.; Cui, Q.; Baboul, A. G.; Clifford, S.; Cioslowski, J.; Stefanov, B. B.; Liu, G.; Liashenko, A.; Piskorz, P.; Komaromi, I.; Martin, R. L.; Fox, D. J.; Keith, T.; Al-Laham, M. A.; Peng, C. Y.; Nanayakkara, A.; Challacombe, M.; Gill, P. M. W.; Johnson, B.; Chen, W.; Wong, M. W.; Gonzalez, C.; Pople, J. A. Gaussian03, Revision E.01; Gaussian, Inc.: Wallingford, CT, 2004.

(40) Dennington, R., II; Keith, T.; Millam, J. GaussView, Version 4.1; Semichem, Inc.: Shawnee Mission, KS, 2007.

(41) Perdew, J. P.; Burke, K.; Ernzerhof, M. *Physical Review Letters* **1996**, *77*, 3865.

(42) Adamo, C.; Cossi, M.; Barone, V. *Journal of Molecular Structure: Theochem* **1999**, *493*, 145.

(43) Perdew, J. P. In *Proceedings of the 21st Annual International Symposium on the Electronic Structure of Solids*; Ziesche, P., Eschrig, H., Eds.; Akademie Verlag: Berlin, 1991.

(44) Adamo, C.; Barone, V. *Journal of Chemical Physics* **1999**, *110*, 6158.

(45) Schultz, N. E.; Staszewska, G.; Staszewski, P.; Truhlar, D. G. *Journal of Physical Chemistry B* **2004**, *108*, 4850.

(46) Zhao, Y.; Schultz, N. E.; Truhlar, D. G. *Journal of Chemical Physics* **2005**, *123*, 161103.

(47) Lynch, B. J.; Zhao, Y.; Truhlar, D. G. *Journal of Physical Chemistry A* **2003**, *107*, 1384.

(48) Lion-XO PC Cluster, http://gears.aset.psu.edu/hpc/systems/lionxo/.

(49) Casey, W. H.; Swaddle, T. W. *Reviews of Geophysics* **2003**, *41*, 1008.

(50) Blum, A. E.; Stillings, L. L. Feldspar dissolution kinetics. In *Chemical Weathering Rates of Silicate Materials*; White, A. F., Brantley, S. L., Eds.; Mineralogical Society of America: Washington, D. C., 1995; Vol. 31; pp 291.

(51) Chen, Y.; Brantley, S. L. *Chemical Geology* **1997**, *135*, 275.

(52) Hellmann, R. *Geochimica et Cosmochimica Acta* **1994**, *58*, 595.

(53) Dissociation Constants of Inorganic Acids and Bases. In *CRC Handbook of Chemistry and Physics*; 88th ed.; Lide, D. R., Ed.; CRC Press/Taylor and Francis: Boca Raton, FL, 2008.

(54) Casey, W. H.; Lasaga, A. C.; Gibbs, G. V. *Geochimica et Cosmochimica Acta* **1990**, *54*, 3369.

(55) Kowall, T.; Caravan, P.; Bourgeois, H.; Helm, L.; Potzinger, F. P.; Merbach, A. E. *Journal of the American Chemical Society* **1998**, *120*, 6569.

Chapter 4: Conclusion

Ab-initio methods are used for dissolution reaction studies, and reaction mechanisms are determined for both Al-O_{br}-Si and Si-O_{br}-Al sites. Protonated and neutral Al-O_{br}-Si sites have lower barrier heights than Si-O_{br}-Al sites. Si-O_{br}-Al sites proceed through nearly identical dissolution reaction mechanisms as Si-O_{br}-Si sites. The computational methods examined repeated the trends from the mechanistic calculations, and the data presented here replicate experimental observations.

The mechanistic analysis performed in this work has several implications. First, the leaching of Al from the mineral surface before Si is in part explained by the differences in barrier heights presented here. Second, the different mechanisms for Si-O_{br}-Al and Si-O_{br}-Si sites show that the non-reacting neighbor site does not affect the reaction progression when Si is the reacting center. Third, the dissolution of each protonation state is different for each type of site. Fourth, additional considerations must be included in future ab-initio studies such as the coordination state of Al-O_{br}-Si sites and the protonation state of clusters.

Several future directions are possible using data from this work, and they are based either on the dissolution of aluminosilicate minerals or the employment of ab-initio methods to determine mechanisms of reactions during dissolution. Initially, the rates of these reactions can be calculated if the surface concentrations of protonation states, the surface stoichiometry of Al-O_{br}-Si and Si-O_{br}-Al sites, and the rate constants of each of these reactions are known.[1] Then the size of the reaction system can be increased using either MC or MD methods, and in fact, the development of MC methods to examine

dissolution of several hundred atoms is already underway.[2] The inclusion of a time parameter as well as the ability to study thousands of particles simultaneously in MD simulations make them useful tools for studying rates of dissolution of aluminosilicate minerals. In particular, the sodium ions which have already been leached from the chemical systems described in Chapter 3 of this work can be included in bulk representations of aluminosilicate minerals using MD simulations to determine if the ab-initio trends are replicated, and an investigation of the coupled dissolution-diffusion model, which poses that dissolution can be affected by the diffusion of chemical species through the leached layer,[3] can be designed using this technique. The development of a MD approach for the investigation of aluminosilicate minerals in particular is possible because of the potentials developed by Zirl and Garofalini.[4]

In addition, mechanistic analyses such as those employed here can be performed using model clusters of other silicate minerals. Two silicate minerals which need mechanistic investigation are borosilicate materials for the remediation of radioactive waste[5,6] and forsterite minerals for the sequestration of carbon dioxide which has been receiving increasing attention in recent years.[7-9] One alternative to the model silicate clusters discussed in this work is the use of metal ions in solution to investigate the means by which minerals dissolve,[10,11] and several researchers are employing this technique with water exchange reactions around metal ions.[12,13]

References

(1) Nangia, S.; Garrison, B. J. *Journal of Physical Chemistry A* **2008**, *112*, 2027.

(2) Nangia, S.; Garrison, B. J., unpublished.

(3) Brantley, S. L.; Stillings, L. *American Journal of Science* **1996**, *296*, 101.

(4) Zirl, D. M.; Garofalini, S. H. *Journal of the American Ceramic Society* **1990**, *73*, 2848.

(5) Ledieu, A.; Devreux, F.; Barboux, P.; Sicard, L.; Spalla, O. *Journal of Non-Crystalline Solids* **2004**, *343*, 3.

(6) Bowers, G. M.; Ravella, R.; Komarneni, S.; Mueller, K. T. *Journal of Physical Chemistry B* **2006**, *110*, 7159.

(7) Giammar, D. E.; Bruant, R. G.; Peters, C. A. *Chemical Geology* **2005**, *217*, 257.

(8) Hanchen, M.; Prigiobbe, V.; Storti, G.; Seward, T. M.; Mazzotti, M. *Geochimica et Cosmochimica Acta* **2006**, *70*, 4403.

(9) Matter, J. M.; Takahashi, T.; Goldberg, D. *Geochemistry Geophysics Geosystems* **2007**, *8*, Q02001.

(10) Casey, W. H.; Swaddle, T. W. *Reviews of Geophysics* **2003**, *41*, 1008.

(11) Helm, L.; Merbach, A. E. *Chemical Reviews* **2005**, *105*, 1923.

(12) Evans, R. J.; Rustad, J. R.; Casey, W. H. *Journal of Physical Chemistry A* **2008**, *112*, 4125.

(13) Olsen, A.; Kubicki, J. D., unpublished.